

**Design and optimisation of OpenStride an open-source inexpensive
force plate actometer**

By

Yang Yang

A thesis submitted to fulfil the requirements
for the degree of Master of Philosophy

School of Biomedical Engineering
Faculty of Engineering

The University of Sydney

2026

Statement of Originality

This is to certify that the content of this thesis is my own work. This thesis has not been submitted for any other degree or purpose.

I certify that the intellectual content of this thesis is the product of my own work, and that all assistance received in preparing this thesis and all sources have been acknowledged.

Yang Yang

24 February 2026

AI attribution statement

During the preparation of this thesis, the author used Microsoft Copilot (University of Sydney protected version) for the purposes of copyediting, including improving sentence clarity, correcting grammar, refining academic language, and enhancing code comment readability.

The author confirms that where text was modified by generative AI, the content was reviewed for possible errors, inaccuracies, and bias. The author takes full responsibility for the submitted thesis and ensures the work is their own and has used generative AI within the parameters of use (refer to the University of Sydney generative AI guide for researchers).

Yang Yang

24 February 2026

Abstract

Quantitative assessment of rodent motor behaviour is central to preclinical neuroscience, and evaluation of naturalistic movement is of particular interest to many researchers. In the early 2000s, force plate actometry (FPA) was developed as an approach to track rodent subject centre-of-mass (COM) with high temporal and spatial precision, enabling varied quantifications relevant to motor performance and behaviour. FPA was commercialised for a period of time, but these systems cost approximately \$15,000 AUD and are no longer produced. Thus, despite clear strong utility particularly in the context of movement disorders and neuropsychiatric research, FPA adoption has remained limited. In this work, we sought to develop an open-source, low-cost FPA system called OpenStride, and to characterise how its performance is shaped by hardware and signal processing choices, with the goal of providing users with the information needed to deploy it effectively across diverse experimental contexts.

First, we designed OpenStride to be able to be fabricated for approximately \$800 AUD using standard 3D printing and laser cutting. We demonstrated that it achieves minimal static drift during long recordings and minimal signal displacement in response to external environmental perturbation. Next, we demonstrated that OpenStride reliably tracks position and distance, and that it can separate groups of rodents with established motor phenotypes. Further, we characterised the influence of five key variables on measurement quality: first, greater applied load improved both static stability and resistance to external perturbation, suggesting that larger subjects will improve signal to noise ratios as expected. Further, each of load cell excitation voltage, mechanical damping, and signal filtering can improve recording quality. Finally, in the context of 3D-printed walking platforms, platform mass had limited impact across the tested range.

Our findings support the interpretation that OpenStride is capable of meaningful motor and behavioural quantification across rodent species and experimental paradigms. Its

performance is influenced by modifiable hardware and software parameters, and understanding these relationships allows users to configure the system to suit their specific needs. All hardware and software will be freely distributed via GitHub, with the intent of making force plate actometry accessible to a broader research community.

Acknowledgement

I wish to express my deepest gratitude to my primary supervisor, Dr Collin Anderson. You changed my life, and I could not have done this without you. When I arrived with no research experience, you guided me with care and thoroughness at every stage. Whenever I encountered difficulty in the laboratory or felt lost in my research direction or writing, you responded with calm and clarity, helping me work through the problem and meeting my mistakes with patience and generosity. Through this process, you not only helped me solve academic challenges but also cultivated in me the ability to think and find my own way forward. You are not only my supervisor but also my role model and my inspiration. I am sincerely grateful for your mentorship and support, which have had a lasting impact on my academic journey.

I would also like to sincerely thank my co-supervisor, Professor Omid Kavehei. Although the nature of the project meant that our direct interactions were less frequent, you were consistently an encouraging presence throughout. You brought openness, optimism, and genuine support to the project, and I am grateful for the role you played and for your generosity throughout.

I also wish to thank my wonderful labmates, Michael, Kajal, Henry, and Sarah, and all our collaborators. In our interdisciplinary team, the diverse backgrounds and experiences each of you brought enriched my thinking and this research in ways I could not have anticipated. Your help with experimental questions, technical challenges, and research discussions was invaluable. Beyond the science itself, the warmth, openness, and mutual support within our group made this a truly meaningful experience. I feel very lucky to have shared this journey with all of you.

I am also grateful to the University of Sydney for providing an outstanding research environment and academic resources that made this work possible. I would particularly like to

thank the staff of Laboratory Animal Services for their essential support for the experimental work. The years I have spent at this university have been among the most formative of my life.

Finally, I want to thank my family and friends. Your unconditional understanding, encouragement, and support gave me the strength to keep going through the hard times. You are, and always will be, where my strength comes from.

To everyone who offered guidance, support, or companionship along the way — thank you, sincerely.

Author Attribution Statement

This thesis contains material from the following manuscript, under review for publication:

Yang Y, Cooper B, Houghton M, Dahiya K, Haslam SE, Blackwell H, Sekaran K, Hu L, Kavehei O, Anderson CJ. OpenStride: an inexpensive, open-source force plate actometry system for quantification of rodent motor activity and behaviour. bioRxiv. 2025:2025.12.17.695041.

Material from this manuscript appears in Chapter 2, Sections 3.3.2 and 3.4.1, and Figure 3.1.

I led the study with primary advising from Dr. Collin Anderson. I led software development in collaboration with Dr. Collin Anderson and developed hardware in collaboration with Michael Houghton and Brock Cooper. I led experiments in collaboration with Michael Houghton, Kajal Dahiya, Sarah Haslam, Henry Blackwell, Kaanchana Sekaran, Lingye, and Dr. Collin Anderson, and I performed data analysis in collaboration with Dr. Collin Anderson. I wrote the drafts of the manuscript, with editorial contributions from all co-authors.

In addition to the authorship attribution statement above, as I am not the corresponding author of this publication, permission to include the published material has been granted by the corresponding author, Dr. Collin Anderson.

Yang Yang,

24/02/2026

As supervisor for the candidature upon which this thesis is based, I can confirm that the authorship attribution statement above is correct.

Dr. Collin Anderson,

Publications

Manuscripts

Yang, Y., Cooper, B., Houghton, M., Dahiya, K., Haslam, S.E., Blackwell, H., Sekaran, K., Hu, L., Kavehei, O., & Anderson, C.J. OpenStride: an inexpensive, open-source force plate actometry system for quantification of rodent motor activity and behaviour. *Scientific Reports* (2026). <https://doi.org/10.1038/s41598-026-44953-z>

Presentations

Poster Presentation

Yang, Y., & Anderson, C.J. (2025). OpenStride: an inexpensive, open-source force plate actometry system for quantification of rodent motor activity and behaviour. Poster presented at the Annual Scientific Meeting of the Australasian Neuroscience Society, Hobart, Tasmania, Australia. December 2025.

Oral Presentation

Yang, Y. (2025). OpenStride: an inexpensive, open-source force plate actometry system for quantification of rodent motor activity and behaviour. Oral presentation at PubTalks: A biomedical science and engineering seminar series, Wentworth Building, The University of Sydney, Sydney, Australia. June 2025.

Table of Content

Chapter 1: Introduction-----	1
1.1 Background and Motivation -----	1
1.2 Modelling neurological disorders in rodents -----	2
1.3 Existing Behavioural and Motor Measurement Systems -----	5
1.4 Force plate actometry-----	11
1.5 Research Gap -----	15
1.6 Research Aims:-----	16
1.7 Scope, Assumptions -----	18
Chapter 2: Aim 1 – Baseline Device Design and Validation-----	21
2.1 Abstract-----	21
2.2 Introduction -----	22
2.3 Methods -----	24
2.3.1 Animals-----	24
2.3.2 Hardware and Software Architecture-----	24
2.3.3 Mechanical stability validation-----	27
2.3.4 Positional accuracy validation-----	27
2.3.5 Locomotor behaviour based on trajectories-----	28
2.3.6 Ataxia and tremor quantification-----	29
2.3.7 Statistical analyses -----	30
2.4 Results -----	31
2.4.1 Mechanical stability and accuracy of position and distance-----	31
2.4.2 Wild-type rodent locomotor validation-----	32
2.4.3 Tremor and ataxia measurements -----	33
2.5 Discussion-----	34
Chapter 3: Aim 2 – Device Optimisation -----	38
3.1 Abstract -----	38
3.2 Introduction-----	39

3.3 Methods	40
3.4 Results	45
3.5 Discussion	53
Chapter 4: Conclusion and Future Work	59
4.1 Overall Summary	59
4.2 Implications of the work	60
4.3 Comparison to other devices	62
4.4 Limitations	64
4.5 Future Directions:	67
4.6 Conclusions	70
5. References	73
Appendix A	81
Figure A.1 OpenStride graphical user interface (main window)	81
Figure A.2 OpenStride data analysis interface	81
Figure A.3 Distance and speed analysis results	82
Figure A.4 LMB analysis results	82
Figure A.5 Tremor analysis results	83
Figure A.6 Ataxia analysis results	83
Appendix B	84

Table of Figure

Figure 1.1	Examples of behavioural measurement methods	11
Figure 1.2	Examples of reported applications of force plate actometry (FPA)	16
Figure 2.1	OpenStride hardware	27
Figure 2.2	Positional accuracy and distance measurement in OpenStride	31
Figure 2.3	Quantification of locomotor activity and behavioural metric.....	32
Figure 2.4	Quantification of ataxia and tremor	33
Figure 3.1	Mechanical stability and drift characterisation of the OpenStride system	44
Figure 3.2	Plate mass versus ataxia ratio measurements in wild-type mouse and rat	45
Figure 3.3	Effect of load cell excitation voltage on distance measurement accuracy	46
Figure 3.4	Effect of damping thickness on positional drift in the OpenStride system	48
Figure 3.5	Effect of signal filtering methods on distance measurement accuracy	50

Figure 1.1 Examples of commonly used rodent behavioural measurement methods. 10

Figure 1.2: Examples of reported applications of force plate actometry (FPA)..... 15

Chapter 1: Introduction

1.1 Background and Motivation

Quantitative analysis of animal behaviour is useful to modern neuroscience, offering a practical readout of nervous system function. In preclinical models, behavioural phenotypes are one method to bridge the gap between therapeutic interventions and clinically relevant outcomes. Consequently, the reliability of preclinical therapeutic innovation could be improved by the precision of behavioural measurement. Objective, quantitative assessment therefore can play a useful role in translational research, ensuring the reproducibility and comparability needed to advance therapeutic developmental studies (Pereira et al., 2020; Perrin, 2014).

Many commonly used behavioural assays continue to rely on manual observation and expert-based scoring, introducing subjectivity and inter-observer variability into behavioural measurement (Isik et al., 2023; Levitis et al., 2009). Such bias can compromise reproducibility across experiments and laboratories. In addition, manual behavioural analysis is inherently time-consuming and does not scale to studies with larger numbers of subjects, limiting experimental throughput (Button et al., 2013; von Ziegler et al., 2021). Addressing these limitations could be accomplished with automated, computational methods for behavioural quantification that provide objective, reproducible measurements independent of observer interpretation (Anderson et al., 2014; et al., 2020).

In response to the need for more objective and automated behavioural measurement, a range of alternative approaches has been explored, including video-based systems, force transducing platforms, and sensor-based tracking. Among these, force plate actometer (FPA) quantifies motor behaviour based on the measurement of ground reaction forces during unconstrained movement. Originally developed by Fowler, Zarcone, and others in the early 2000s, FPA systems track centre-of-mass (COM) trajectories from force signals to provide a measure of locomotor activity with high resolution, both spatially and temporally (Fowler et

al., 2001). Subsequent studies demonstrated the utility of FPA for quantifying movement distance and detecting hyperactivity in genetic mouse models, such as those with altered dopaminergic function and neurotrophin overexpression (Fowler, Zarcone, Chen, et al., 2002; Fowler, Zarcone, Vorontsova, et al., 2002). These early applications established FPA as a viable tool for objective behavioural phenotyping in rodents. Recent work from Anderson and colleagues has taken advantage of FPA-based analyses in the context of frequency-domain and trajectory-regularity measures, quantifying tremor, straightness of gait, and grooming behaviours associated with neurological dysfunction. Specifically, FPA has been applied to studies of deep brain stimulation (Anderson et al., 2019), gene identification (Figuerola et al., 2023), gene therapeutic development (Anderson et al., 2025), and novel mouse models of Tourette syndrome (Anderson et al., 2024). Thus, FPA is a flexible tool for quantifying multiple aspects of rodent motor activity and behaviour.

Despite the demonstrated utility of force plate actometry for quantitative motor phenotyping, its adoption as a routine behavioural measurement tool has remained modest, and the original FPA system is no longer commercially available. This project is therefore motivated by the need to adapt force plate actometry into an accessible form well suited for experimental use. Thus, we developed the open-source tool OpenStride, aiming to generate a new open-source, cost-effective, easily produced FPA platform that supports high-resolution, automated, and objective behavioural measurement across a wide range of research settings.

1.2 Modelling neurological disorders in rodents

Neurological disorders encompass a broad spectrum of conditions that impair functional independence and quality of life. These conditions are often categorised into major, overlapping domains of dysfunction, such as neuropsychiatric, movement, sensory, and autonomic, the first two of which are highly relevant to force plate actometric measurement

when modelled in rodents. Neuropsychiatric disorders, such as anxiety, depression, obsessive-compulsive disorder (OCD), attention-deficit/hyperactivity disorder (ADHD) and Tourette syndrome, are primarily characterised by alterations in affect, cognition, and repetitive behaviours (First, 2013). Conversely, movement disorders, such as Parkinson's disease, essential tremor, or cerebellar ataxias, are often defined by the degradation of motor control, coordination, and stability (Baker, 2018; Goetz et al., 2008; Tanner et al., 2024). In this section, we detail approaches in modelling neuropsychiatric and movement disorders in rodents.

Rodent models of neuropsychiatric dysfunction have been established through diverse approaches, including natural occurrence, genetic manipulation, pharmacological intervention, and selective breeding. These models typically exhibit alterations in anxiety-like behaviour, compulsive actions, activity levels, and social interactions (Nestler et al., 2010). From a measurement perspective, neuropsychiatric models predominantly manifest as changes in behavioural choice and spatial patterns, where animals move, how much they move, and how they interact with their environment, rather than deficits in the quality of motor execution itself. Models of anxiety and depression frequently co-occur in their behavioural phenotypes, generated through diverse approaches (Carlezon et al., 2005; Krishnan et al., 2007; Wallace et al., 2009), including genetic manipulations, chronic stress paradigms, and early life adversity (Gururajan et al., 2019). These models typically present with altered exploratory behaviour, changes in total locomotor activity, and modified spatial preferences between open versus enclosed spaces, phenotypes that are readily quantifiable through trajectory-based analysis of where and when movements occur. Repetitive behaviour disorders, including OCD and related conditions, are characterised by stereotyped action sequences that differ from typical locomotor patterns. OCD is modelled through genetic deletions affecting cortico-striatal circuits, including SAPAP3 and SLITRK5 knockout mice, both of which exhibit excessive self-grooming and repetitive behaviours responsive to chronic fluoxetine treatment (Shmelkov et

al., 2010; Welch et al., 2007). These stereotypies represent spatially constrained, rhythmic movement patterns that can be distinguished from exploratory locomotion through temporal and spatial analysis of movement trajectories. Hyperactivity disorders present distinct measurement challenges, characterised by elevated locomotor activity and altered impulse control. ADHD is modelled in spontaneously hypertensive rats and dopamine transporter knockout mice, displaying hyperlocomotion and impulsivity assessed through activity monitoring and operant tasks (Sagvolden et al., 2005). Tourette syndrome has been modelled through genetic manipulations such as D1CT-7 transgenic mice and through autoimmune mechanisms via intrastriatal infusion of sera from patients with high autoantibody levels (Godar et al., 2016; Taylor et al., 2002). Both conditions require measurement systems capable of detecting elevated baseline activity while resolving brief, stereotyped movements superimposed on locomotor behaviour. Collectively, rodent models of neuropsychiatric disorders present measurement requirements centred on spatial exploration patterns, total activity levels, and detection of repetitive or stereotyped behaviours. Unlike movement disorders that affect motor execution quality, these models require analytical approaches that capture where animals move, how frequently they move, and whether movement patterns become stereotyped—measurement dimensions that can be addressed through trajectory-based analysis of centre-of-mass position over time.

Rodent models of movement disorders are characterised by various deficits in motor execution quality, replicating tremor, bradykinesia, and ataxia observed in human movement disorders through varied approaches, such as genetic mutations, neurotoxic lesions, or spontaneous mutations affecting motor control circuits (Kuo et al., 2019). Pharmacological models, neurotoxic lesion models, and genetic models are commonly used to study Parkinson's disease. These include pharmacological approaches such as reserpine or haloperidol, neurotoxic lesions using 6-hydroxydopamine (6-OHDA) or

1-methyl-4-phenyl-1,2,3,6-tetrahydropyridine (MPTP), and genetic models involving mutations in genes such as SNCA, LRRK2, and PRKN (Duty et al., 2011). These models exhibit bradykinesia, postural instability, and in some cases tremor. Tremor-dominant motor phenotypes, including postural and kinetic tremor characteristic of essential tremor, have been modelled in harmaline-treated rodents and in genetic models with cerebellar dysfunction (Handforth et al., 2001; Kuo et al., 2019; Welton et al., 2021). Further, cerebellar ataxia can be modelled through various genetic mutations affecting cerebellar development or function, toxin-based models such ethanol induction, or stereotactic lesion. These models exhibit irregular gait, impaired coordination, and postural instability (Figuroa et al., 2023; Funato et al., 2021; Hansen et al., 2013; Tejwani et al., 2024; Wang et al., 2024).

Collectively, rodent models of neuropsychiatric and movement disorders provide experimental platforms that recapitulate key behavioural and motor phenotypes. Neuropsychiatric models manifest alterations in spatial preferences, exploratory patterns, and repetitive behaviours, while movement disorder models exhibit deficits in motor execution quality including tremor, gait irregularity, and coordination impairments. The diversity of required measurements across these models motivates the need for flexible measurement platforms capable of capturing both spatial and kinematic phenotypes, a challenge addressed in the subsequent sections reviewing existing measurement approaches and their limitations.

1.3 Existing Behavioural and Motor Measurement Systems

A variety of methods have been developed for the assessment of behavioural and motor function in rodents. Video-based systems track movement through optical recording and enable behavioural analysis via manual scoring or automated computer-vision methods (Mathis et al., 2018; Noldus et al., 2001). They are commonly used to quantify spatial exploration, activity patterns, and selected kinematic parameters. Dedicated motor assessment devices, including

the rotarod (Dunham et al., 1957; Jones et al., 1968), treadmill (Guillot et al., 2008), elevated beam (Luong et al., 2011), and Erasmus ladder (Vandeputte et al., 2010), are designed to probe specific motor functions such as balance, coordination, and gait. In addition, sensorimotor paradigms such as prepulse inhibition (PPI) assess neural circuit function through reflex-based responses (Swerdlow et al., 2008). Below, we detail several standard approaches.

1.3.1 Motor Assessment Systems

Manual video analysis is a traditional approach to behavioural quantification, in which trained observers score behaviours from recorded footage. This method offers high interpretability and experimental flexibility, enabling detailed characterisation of complex and context-dependent behaviours, including grooming sequences, social interactions, and rare or irregular actions that remain challenging to automate (Crawley, 2007). However, manual analysis is labour-intensive and time-consuming and is subject to inter-observer variability that can compromise reproducibility across studies and laboratories (Anderson et al., 2014).

Automated video tracking systems address some limitations of manual analysis by using computer vision algorithms to extract movement trajectories and behavioural metrics. Commercial platforms such as EthoVision (Noldus et al., 2001) track body location and basic activity parameters, while recent open-source machine learning approaches including DeepLabCut (Mathis et al., 2018) and SLEAP (Pereira et al., 2022) enable marker less pose estimation for detailed kinematic analysis. These systems offer quantification of spatial parameters, distance travelled, and velocity. However, video-based approaches face inherent limitations: they require line-of-sight visibility, are sensitive to lighting conditions and occlusions, and typically cannot resolve fine-grained force dynamics or high-frequency motor features such as tremor without additional sensors (Mathis et al., 2020).

The rotarod assesses motor coordination and balance by measuring the latency for a rodent to fall from an accelerating or constant-speed rotating cylinder (Dunham et al., 1957;

Jones et al., 1968). This paradigm is widely used to evaluate motor impairments in models of cerebellar ataxia, Parkinson's disease, and other movement disorders (Carter et al., 2001). The rotarod provides a simple readout of gross motor function. However, it measures only a single composite endpoint (latency to fall) and does not capture the kinematic details of movement or gait characteristics. Additionally, performance can be influenced by anxiety-like behaviours and motivation rather than purely motor deficits (Brooks et al., 2009; Carter et al., 1999). Notably, rotarod requires training sessions to establish stable baseline performance, and results can be affected by experimenter handling and inter-rater variability in determining the precise moment of fall (Brooks et al., 2009; Deacon et al., 2006; McFadyen et al., 2003; Rustay et al., 2003).

The elevated beam test evaluates balance and fine motor coordination by measuring the ability of rodents to traverse a narrow beam suspended above the ground, with outcomes including traversal time, number of foot slips, and falls (Luong et al., 2011). This paradigm is sensitive to cerebellar dysfunction, basal ganglia lesions, and other motor impairments (Bidgood et al., 2024; Piotrowski et al., 2024; Sawers et al., 2015). The elevated beam provides a straightforward assessment of balance and coordination with minimal equipment requirements. However, like the rotarod, it yields composite scores that do not capture detailed movement kinematics, and performance can be confounded by anxiety-related avoidance of the elevated, open apparatus (Carter et al., 2001).

Treadmill-based gait analysis quantifies locomotor patterns by recording animals walking or running on a moving belt, typically combined with high-speed video or pressure sensors to extract gait parameters such as stride length and stance time (Guillot et al., 2008). This approach enables kinematic assessment and has been applied to varied models, such as spinal cord injury, peripheral neuropathy, and motor neuron disease (Harnie et al., 2019; Maier et al., 2009; Neckel et al., 2008; Wooley et al., 2005). Treadmill systems provide reproducible

locomotor contexts and can reveal subtle gait abnormalities. However, the constrained, forced locomotion may not reflect naturalistic movement patterns, and some animals require extensive training or show reluctance to ambulate on the treadmill, potentially introducing selection bias (de Assis et al., 2024; Herbin et al., 2007)

The Erasmus ladder is an automated gait analysis system in which rodents traverse a horizontal ladder with rungs that can be raised or lowered to create perturbations, enabling assessment of adaptive motor control and motor learning (Vandeputte et al., 2010; Vinueza Veloz et al., 2012). The system records stepping patterns, rung contacts, and responses to unexpected obstacles, providing insights into both baseline gait and adaptive motor strategies (Vinueza Veloz et al., 2015). The Erasmus ladder offers kinematic data. However, it requires specialised equipment, extensive training protocols, and interpretation of complex multi-dimensional datasets (Dijkhuizen et al., 2024). Additionally, the constrained linear path may not capture exploratory behaviours or spatial navigation relevant to some neuropsychiatric phenotypes (Sathyanesan et al., 2019; Vinueza Veloz et al., 2015).

1.3.2 Behavioural and Cognitive Assessment Systems

Beyond motor function described above, a variety of paradigms have been developed to assess non-motor behaviours, including sensorimotor gating, spatial cognition, and affective states relevant to rodent models of neuropsychiatric disorders. These approaches typically rely on choice behaviour or reflex-based responses rather than continuous motor performance and provide functional readouts of neural circuit integrity and behavioural state.

Prepulse inhibition (PPI) assesses sensorimotor gating by measuring the reduction in startle response when a weak pre-stimulus precedes a stronger startle-eliciting stimulus (Swerdlow et al., 1994). PPI deficits are observed across multiple neuropsychiatric disorders, such as schizophrenia, Tourette syndrome, and OCD. (Jafari et al., 2020; Kohl et al., 2013). PPI provides a circuit-level functional readout that is reproducible and amenable to

pharmacological validation. However, it does not directly measure motor execution or locomotor activity, and abnormalities in PPI may reflect diverse underlying mechanisms, including attention, arousal, or circuit dysfunction, rather than a specific behavioural phenotype (Kilts, 2001; Swerdlow, 2013).

The Y-maze and T-maze assess spatial working memory through spontaneous or rewarded alternation paradigms, in which rodents explore maze arms and performance is quantified by alternation rates or choice accuracy (Deacon et al., 2006). These paradigms are widely used to evaluate cognitive deficits in models of Alzheimer's disease, schizophrenia, and ADHD. Maze-based tests provide straightforward behavioural readouts with minimal training requirements. However, they capture only discrete choice behaviour rather than continuous motor kinematics, and performance can be influenced by locomotor activity, anxiety, and motivational state (Lalonde, 2002).

The forced swim test (FST) and tail suspension test (TST) assess depression-like behaviour by measuring immobility time when rodents are placed in inescapable stressful situations (a water-filled cylinder or suspended by the tail) (Porsolt et al., 1977; Steru et al., 1985). These tests are widely used for antidepressant screening. They provide simple behavioural despair readouts. However, they capture only passive coping responses during acute stress rather than sustained behavioural alterations and do not assess locomotor patterns, spatial behaviour, or motor execution quality (Cryan et al., 2002).

Taken together, existing behavioural and motor assessment methods for rodents encompass a diverse set of paradigms that differ in sensing modality, analytical focus, and the behavioural dimensions they capture. Video-based systems primarily quantify spatial trajectories, activity levels, and pose-defined kinematics, whereas task-constrained motor assays such as the rotarod, treadmill, elevated beam, and Erasmus ladder probe specific aspects of balance, coordination, gait, and motor learning. Reflex-based paradigms such as prepulse

inhibition (PPI) provide reproducible measures of neural circuit function related to sensorimotor gating. Each approach offers advantages for interrogating phenotypes, while simultaneously imposing constraints on the types of behaviour that can be observed and quantified.







Method	Primary Readout	Behavioural Domain	Strengths	Practical Considerations
 Manual behavioural scoring	Optical recording	Activity levels / behaviours	<ul style="list-style-type: none"> • Flexible • Naturalistic 	<ul style="list-style-type: none"> • Time-intensive • Subject to inter-rater variability
 Video tracking	Optical + computer vision	Activity levels / behaviours	<ul style="list-style-type: none"> • Objective • Quantitative 	<ul style="list-style-type: none"> • Sensitive to lighting • Complex setup
 Rotarod/ Elevated Beam	Rotating / elevated apparatus	Fall latency / Traversal metrics / Foot slips	<ul style="list-style-type: none"> • Simple • Sensitive to gross deficits 	<ul style="list-style-type: none"> • Require training • Anxiety/ motivation confounds
 Treadmill/ Erasmus Ladder	Moving belt / perturbable ladder	Step patterns / Adaptive responses	<ul style="list-style-type: none"> • Controlled locomotion • multi-parameter output 	<ul style="list-style-type: none"> • Single composite endpoint • Anxiety/ motivation confounds
 Prepulse inhibition	Acoustic startle chamber	Sensorimotor gating	<ul style="list-style-type: none"> • Circuit-level readout 	<ul style="list-style-type: none"> • Does not assess voluntary locomotion
 Y-T-Maze FST/TST	Maze / stress exposure	Working memory / affective state	<ul style="list-style-type: none"> • Simple • Minimal training 	<ul style="list-style-type: none"> • No spatial/ motor assessment • Anxiety/ motivation confounds

Figure 1.1 Examples of commonly used rodent behavioural measurement methods

1.4 Force plate actometry

The measurement systems reviewed above each demonstrate capabilities and limitations, with individual methods optimised for specific phenotypic features. While this diversity reflects the multifaceted nature of behavioural phenotyping, it also raises the question of whether any approach can provide broad applicability across multiple phenotypic domains while maintaining measurement accuracy and experimental throughput. FPA, the focus of this thesis, represents an approach with the potential to capture diverse behavioural and motor features within a unified measurement context. To evaluate this potential and understand both the capabilities and practical barriers associated with this method, this section reviews the historical development of the FPA, its demonstrated applications across experimental contexts, and some challenges that have limited its widespread adoption.

FPA was introduced by Fowler, Zarcone, and colleagues in the early 2000s (Fowler et al., 2001). The system consists of a rigid platform mounted on four force transducers or load cells. As the animal moves within the chamber, its COM is calculated from the forces applied to each transducer. This approach enables continuous, high-resolution tracking of COM trajectories during unconstrained, naturalistic movement. Unlike video/vision-based systems that rely on optical tracking of body, FPA directly measures the mechanical forces generated by the animal, providing a method for behavioural quantification that is insensitive to lighting conditions and contrast or visual occlusions.

Force plate actometry features several characteristics advantageous for behavioural measurement. First, FPA provides objective, continuous quantification of movement without requiring manual scoring or visual observation, eliminating inter-observer variability. Second, the high temporal resolution of force measurements enables detection of rapid motor events, including tremor oscillations and fine-grained kinematic features that may be difficult to

resolve with standard video frame rates. Third, FPA captures movement in a naturalistic, open-field context without physical restraint or forced locomotion, allowing assessment of spontaneous exploratory behaviour alongside motor execution quality. Fourth, the system simultaneously supports multiple analytical approaches: trajectory-based metrics for spatial exploration and activity patterns, frequency-domain analyses for tremor quantification, and temporal analyses for identifying discrete behavioural bouts such as grooming (Zarcone, 2022).

Following the initial description of FPA, Fowler and Zarcone systematically demonstrated its utility across diverse experimental contexts, establishing FPA as a versatile approach for behavioural neuroscience. Early applications quantified locomotor activity and hyperactivity in genetic mouse models, including those with altered dopaminergic function through D2 dopamine receptor knockout and neurotrophins overexpression, demonstrating FPA's sensitivity to activity-related phenotypes and motor deficits (Fowler, Zarcone, Chen, et al., 2002; Fowler, Zarcone, Vorontsova, et al., 2002). Subsequent work extended FPA-based analyses beyond locomotion to capture fine-grained motor features. Fowler and colleagues developed frequency-domain and trajectory-regularity metrics to quantify tremor and gait irregularity and applied these methods to characterise amphetamine-induced behavioural sensitisation through changes in head movement rhythms during focused stereotypies (Fowler et al., 2003). These analytical extensions demonstrated that FPA could resolve high-frequency motor events and repetitive behavioural patterns that would be difficult to quantify through traditional observation methods. The flexibility of FPA was further illustrated through applications to pharmacological, developmental, and cognitive domains. Fowler and colleagues assessed the effects of methylphenidate on novelty exploration and spatial stimulus preferences, revealing that psychostimulants attenuate rodents' preference for novel spatial stimuli in familiar environments (Fowler et al., 2010). Levant employed FPA to investigate developmental effects of dietary n-3 fatty acid manipulation on activity and response to novelty,

as well as age-dependent differences in methylphenidate dose-response relationships between periadolescent and adult rats (Levant et al., 2011; Levant et al., 2010). These studies established FPA as a tool for assessing both acute pharmacological effects and long-term developmental influences on behaviour. Additional applications explored operant conditioning and response patterns under controlled reinforcement schedules. Fowler and colleagues integrated the FPA with an operant chamber to examine schedule-controlled responding in rats, illustrating how FPA can be combined with complementary behavioural measurement systems to enrich behavioural characterisation (Fowler et al., 2009). Related quantitative force-based approaches have similarly been applied to operant contexts, capturing subtle changes in response vigour and effort allocation in food-maintained responding (Zarcone et al., 2009). These studies extended FPA's applicability to questions of motivation, effort, and behavioural economics. FPA can capture diverse motor and behavioural phenotypes across multiple experimental paradigms, species (mice, rats, and voles), and research domains, from locomotor activity and stereotypy to cognitive function and operant behaviour (Fowler et al., 2007; Hövel et al., 2019; Russell et al., 2013; Tao et al., 2015; Tickerhoof et al., 2020). The breadth of these applications demonstrated that force-based measurement could serve as a broadly applicable tool for addressing questions spanning motor control, neuropsychiatric function, pharmacology, and development.

Alongside these studies, FPA was also increasingly adopted in application-driven research to address specific experimental questions and disease-related phenotypes. For neuropsychiatric phenotypes, FPA has been applied to characterise sensorimotor gating deficits and behavioural responses to environmental manipulation in Tourette syndrome models, for example. In D1CT-7 transgenic mice, FPA quantified altered spatial exploration patterns and activity levels during exposure to spatial confinement (Godar et al., 2016). FPA-based activity measures, including distance travelled, time spent in defined zones, and movement velocity,

have been employed to assess steroid hormone effects on dominance-related behaviours and impulse control (Mosher et al., 2018) and combined with prepulse inhibition paradigms to examine neurosteroid modulation of sensorimotor gating (Mosher et al., 2019). Recent work has explored methodological extensions, applying machine learning approaches to force-based trajectories for automated classification of complex grooming behaviours (Anderson et al., 2024). For motor disorders, FPA has been employed to characterise cerebellar dysfunction in the *shaker* rat model of ataxia, quantifying tremor through power spectral density analysis of signals and ataxia through trajectory-regularity ratios (path length divided by net displacement). These tremor and ataxia metrics served as primary outcomes for evaluating deep cerebellar stimulation efficacy (Anderson et al., 2019) and have also been applied to the genetic characterisation of Slc9a6-mediated Purkinje cell degeneration (Figueroa et al., 2023), as well as to the assessment of viral gene replacement therapies for Christianson syndrome (Anderson et al., 2025). These applications illustrate FPA's versatility for quantifying diverse phenotypes through frequency-domain, trajectory-based, and computational analytical approaches.

The historical development and applications reviewed above show that force plate actometry (FPA) has been used to measure locomotor activity, tremor-related oscillations, and repetitive behaviours across multiple experimental models. The platform records force signals continuously and allows extraction of both trajectory-based behavioural measures (e.g., spatial exploration and activity levels) and frequency-domain motor features (e.g., tremor-associated oscillations) within a single recording session. Unlike task-based paradigms, FPA recordings do not require explicit training procedures or externally cued task performance. The system generates quantitative outputs that can be analysed at different temporal scales. Reported applications include locomotor profiling, tremor detection, and algorithm-based behavioural classification. At the same time, the practical implementation of FPA has been shaped by considerations related to system availability, cost, and software infrastructure. Early and

subsequent implementations reported in the literature have relied on specialised hardware configurations and proprietary software environments, factors that influence accessibility, customisation, and ease of deployment across laboratories. These considerations provide important context for understanding the scope and limitations of FPA use to date.

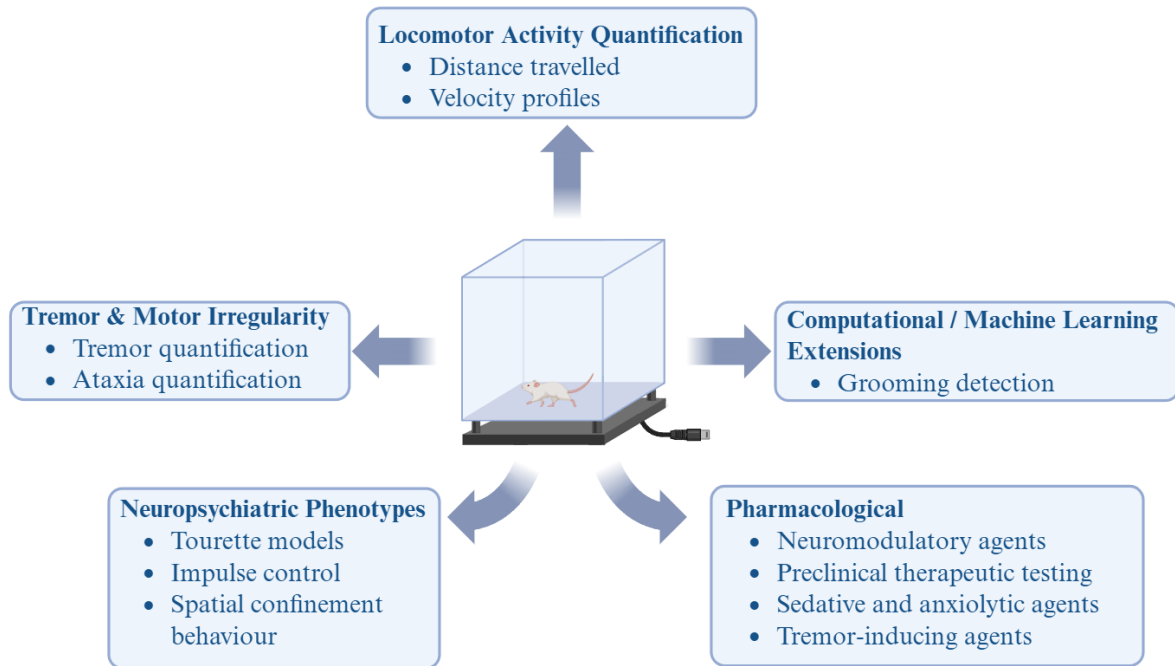


Figure 1.2: Examples of reported applications of force plate actometry (FPA)

1.5 Research Gap

While the scientific literature documents diverse applications of FPA across motor disorders, neuropsychiatric models, and pharmacological studies, the availability of mature, user-ready FPA systems is limited. The original FPA systems are no longer commercially available, and alternatives have not emerged to fill this gap. As a result, recent studies employing FPA have largely relied on legacy hardware and software configurations that are no longer actively maintained. Consequently, laboratories seeking to adopt FPA face barriers, including the absence of readily available hardware designs, a lack of access to validated and

actively supported software environments, and insufficient documentation for system construction, operation, and data analysis. Commercial FPA systems require compatibility with legacy operating systems, while recently reported analytical workflows for extracting key behavioural and motor metrics frequently rely on external, custom-written MATLAB scripts rather than integrated software pipelines. Together, these factors increase the technical burden associated with FPA deployment and limit accessibility for researchers without engineering or computational backgrounds.

The entry point for this work lies at the intersection of three critical needs: (1) the scientific need for objective, high-resolution motor phenotyping in rodent models of neurological disorders; (2) the practical need for accessible and affordable measurement paradigms that can be deployed across laboratories using standard fabrication capabilities; and (3) the methodological need for transparent and customisable systems that support iterative refinement and community validation. By prioritising open-source hardware designs, readily available components, and modular software architecture, this project aims to transform the FPA from a specialised technique accessible to a limited number of laboratories into a more broadly available tool. The resulting system, herein called OpenStride, is designed to preserve the core advantages of traditional FPA systems—objectivity, high temporal resolution, and analytical flexibility—while directly addressing the accessibility and reproducibility barriers that have constrained wider adoption.

1.6 Research Aims:

We set out to accomplish 2 specific aims.

Aim 1: Design, construct, and validate an open-source force plate actometry system with sufficient resolution to quantify locomotor activity, tremor, and gait regularity in rodent models.

Aim 2: Determine how to optimise system performance through systematic evaluation of design parameters and iterative refinement of hardware, signal processing, and analytical methods.

Aim 1 encompasses (1) hardware design and fabrication of a force-sensing platform using readily available components and standard manufacturing processes (3D printing, laser cutting); (2) development of data acquisition and real-time processing software compatible with cross-platform operating systems; (3) use of time vs position tests to establish system stability and positional accuracy under dynamic loading and finger tracing tests; and (4) biological validation using wild-type and ataxic rodent models to demonstrate the system's ability to detect established motor activity, such as tremor strength and ataxic movement. Success criteria for this aim include achieving positional accuracy within ± 2 mm across the workspace, maintaining drift below 500 μm during extended recordings, resolving tremor frequencies in the 3–12 Hz range, and detecting significant differences between wild-type and *shaker* rats in ataxia and tremor metrics consistent with prior FPA literature.

Aim 2 encompasses (1) parametric investigation of factors influencing measurement stability and signal-to-noise ratio, including subject mass, platform mass, load cell voltage supply, and mechanical damping; (2) evaluation of signal processing approaches—including temporal smoothing, filtering methods, and sampling rate optimisation, to balance trajectory fidelity with noise reduction; (3) assessment of system robustness to external mechanical perturbations and environmental factors that may impact data quality; and (4) documentation of optimal configurations and operational parameters to guide future users in system

deployment and customisation. Success criteria for this aim include characterisation of load-dependent stability across the rodent mass range (20-500 g), identification of damping configurations that substantially attenuate external perturbations, and establishment of filtering parameters that balance trajectory accuracy with noise reduction for both trajectory-based and frequency-domain analyses.

1.7 Scope, Assumptions

The scope of this work is bounded by several design and experimental constraints that define the project's focus and deliverables. First, hardware development is constrained to components and manufacturing processes accessible to standard academic research laboratories, specifically 3D printing (fused deposition modelling with PLA), laser cutting (acrylic), and commercially available electronic components (load cells, data acquisition interfaces). This constraint ensures reproducibility but excludes higher-precision manufacturing approaches (e.g., CNC machining, custom sensor fabrication) that may offer performance advantages. Second, the experimental validation is limited to mice and rats, with primary emphasis on motor phenotypes (tremor, ataxia, locomotor activity) explored in the *shaker* rat model of cerebellar dysfunction and wild-type controls available to our laboratory group during the completion of this thesis. While the system is designed to support broader applications, comprehensive validation across diverse neuropsychiatric models, developmental stages, or other species is beyond the current scope. Third, all recordings are restricted to single-animal sessions, as conventional FPA provides a single composite force signal and cannot reliably disentangle the contributions of multiple animals within the same chamber. Fourth, software development prioritises core functionality (data acquisition, real-time visualisation, basic analysis) compatible with both Windows and macOS operating systems, with advanced

analytical features (e.g., machine learning-based behaviour classification, automated grooming detection) deferred to future work. Fifth, the project focuses on establishing a functional, validated baseline system rather than exhaustive comparison against all existing behavioural measurement platforms, with direct comparisons limited to established FPA benchmarks from prior literature.

Several design assumptions and associated limitations shape the interpretation and generalisability of this work. First, the system assumes that COM trajectories derived from ground reaction forces provide a sufficient representation of rodent behaviour for the target phenotypes (locomotor activity, tremor, ataxia, spatial exploration). This assumption is supported by extensive prior FPA literature but inherently limits the resolution of fine-grained limb kinematics, postural dynamics, or three-dimensional movements that may be captured by other approaches (e.g., multi-camera videography, marker-based motion capture). Second, the use of lower-cost load cells relative to research-grade force transducers introduces trade-offs between system affordability and signal-to-noise ratio. While the selected components (Teda Huntleigh 1004 series) provide adequate performance for the target applications, they yield higher baseline noise than the precision transducers used in original Fowler-designed systems, potentially limiting sensitivity to subtle motor features in lightweight subjects (e.g., young mice). Third, the open-field, unconstrained measurement context provides naturalistic behavioural assessment but precludes controlled manipulation of specific motor challenges (e.g., obstacle negotiation, precise reaching, skilled forelimb tasks) that can be evaluated with specialised apparatus such as the Erasmus ladder or treadmill-based paradigms. Fourth, the system's reliance on a planar force-sensing surface constrains measurements to a two-dimensional workspace, precluding direct quantification of vertical behaviours (rearing, jumping) beyond their ground reaction force signatures. Finally, while the open-source design facilitates reproducibility and customisation, system performance may vary across

implementations due to differences in component sourcing, manufacturing precision (e.g., 3D printer calibration), and assembly procedures, necessitating local validation and calibration protocols. However, with appropriate documentation, such as version-controlled repositories, white papers, and peer-reviewed publication, calibration processes can be developed to guide users in replicating devices to specified tolerances.

2.1 Abstract

Introduction: Force plate actometry (FPA) enables quantitative assessment of rodent motor and behavioural activity. Through tracking centre of mass at high temporal and spatial resolution, FPA can directly quantify motor performance and various behaviours in the context of operator-independent, naturalistic movement. Previously designed systems have been expensive and non-customisable, and they are no longer commercially available.

Methods: We designed OpenStride, an open-source FPA system consisting of both hardware and software. Our system was designed to be able to be constructed with standard tools worldwide at a cost of ~\$800 AUD, with modifiable hardware files, modular software, and support for both Mac and Windows operating systems, with scope for further platform adaptation. Required tools include 3D printing and acrylic laser cutting.

Results: OpenStride reliably tracks position within a $30 \times 30 \text{ cm}^2$ environment. Based on these positional data, OpenStride currently quantifies tremor, ataxia, distance, velocity, low-mobility bouts, and centre-vs-margin time, with potential to expand to additional analyses.

Conclusions: OpenStride is intended to provide a valuable tool for high-throughput, inexpensive study of motor and behavioural function and dysfunction. Software and hardware files will be freely disseminated online via GitHub at the time of final publication to enable others to construct and utilise the OpenStride system.

2.2 Introduction

Force plate actometry, first published on in 2001, generates the ability to track and analyse naturalistic movement and behaviour in rodents with high spatial and temporal precision (Fowler et al., 2001). A typical force plate actometer (FPA) consists of a stiff platform mounted on four force transducers or load cells; as the subjects ambulates through the chamber, its centre of mass is calculated by the weighted averages of forces applied to each transducer. Coupled with both real-time and post-experimental analyses, this enables the study of a variety of simple and complex behaviours and movements across a large variety of applications (Zarcone, 2022).

Since its initial publication, force plate actometry has been used to study numerous models of various disorders, particularly in the context of neuroscience, psychology, pharmacology, and biomechanics (Figuroa et al., 2023; Godar et al., 2016; Hein et al., 2012; Kuo et al., 2019; Lang et al., 2020; Levant et al., 2011; McCarson et al., 2019; Mosher et al., 2019; Mosher et al., 2018; Scoles et al., 2022; Zarcone et al., 2009), spanning several species, including mice, rats, voles, pigeons, and humans (Crosland et al., 2005; Pinkston et al., 2008; Tickerhoof et al., 2020; Zarcone, 2022). Across this range of models and species, specific measurements made have included distance travelled, rearing, neurodevelopmental phenotypes, operant conditioning, exploration of novelty, stereotypies, ataxia, and tremor (Fowler et al., 2003; Fowler et al., 2010; Levant et al., 2011; Levant et al., 2010; Zarcone, 2022).

We have utilised force plate actometry repeatedly in recent years. First, we combined hardware modified from that initially developed by Fowler with custom software to quantify ataxia, tremor, and falls in the Wistar Furth *shaker* rat, before evaluating deep brain stimulation targeting the deep cerebellar nuclei for degenerative cerebellar ataxia and tremor (Anderson et al., 2019; Lang et al., 2020). Next, we utilised a similar setup to perform automated open-field experiments, studying the effects of *Stau1* knockdown in the context of targeting this gene

therapeutically to treat amyotrophic lateral sclerosis and spinocerebellar ataxia type 2 (Scoles et al., 2022). Subsequently, we used force plate actometry to demonstrate changes associated with functional complementation to prove causality of *Slc9a6* mutation in the *shaker* rat, linking it to Christianson syndrome (Figueroa et al., 2023). More recently, we have combined actometry with machine learning to automate the detection of complex grooming behaviours (Anderson et al., 2024). Finally, we utilised actometry to evaluate viral gene therapies for Christianson syndrome in the *shaker* rat (Anderson et al., 2024). Collectively, this body of work has led us to find actometry to be a highly versatile and reliable approach for sophisticated behavioural and motor quantification.

Previous generations of force plate actometers have several limitations. First, systems are no longer produced or commercially available. Second, costs remained relatively high, limiting uptake in a high-throughput manner. Third, given proprietary software, open-source capabilities to add analyses were not readily present. Thus, we sought to design a novel, inexpensive, open-source force plate actometry system. In this work, we report on our efforts to develop a novel force plate actometry design based on the goals of minimising cost, designing software and hardware in an open-source fashion, ensuring easily reproducible manufacturing, and maximising reliability. To this end, we sought to utilise readily available or easily manufactured components, primarily those that can be assembled on inexpensive 3D printers, while also creating open-source software that can be used with both Mac and Windows operating systems. In total, our cost to produce the new force actometer was approximately \$800 AUD.

2.3 Methods

2.3.1 Animals

All procedures involving animals were approved by the University of Sydney Animal Ethics Committee (protocols 2023/AE002319 and 2024/AE002517) and performed in accordance with the Australian Code for the Care and Use of Animals for Scientific Purposes as well as the Animal Research Act 1985. In total, one adult mouse and 13 adult rats were utilised in this chapter. In both instances, rodents were housed 2-5 per cage under a standard 12:12 hour light cycle and given access to food and water *ad libitum*. The mouse utilised was of the C57BL/6 background, and the 13 rats utilised were Wistar Furth, including 7 wild-type and 6 *shaker* rats hemizygous (male) or homozygous (female) for a loss-of-function mutation in the *Slc9a6* gene, which yields progressive cerebellar degeneration and ataxia (Figuroa et al., 2023).

2.3.2 Hardware and Software Architecture

The OpenStride system consisted of a rigid 3D-printed base supporting a $30 \times 30 \text{ cm}^2$ 3D-printed walking surface enclosed within a 5-mm acrylic chamber. Four single-point load cells (Tedeo Huntleigh Model 1004-00.3-JW00-RS) were mounted beneath the walking platform in a square configuration. STL files for all printed components, acrylic cutting templates, and assembly schematics will be released GitHub at the time of final publication. A $35 \times 35 \times 5 \text{ cm}$ concrete paver was positioned beneath the base, on top of ethylene-vinyl acetate (EVA) foam, under each corner to shield the system from external perturbation and improve its mechanical stability. Hardware design files and software source code are publicly available and detailed in Appendix B.

Each load cell transmitted analogue differential signals to a PhidgetBridge 1046_0B interface, which relayed digitised voltage values to a computer via USB. Real-time acquisition

was implemented in Python using the Phidget21 API, with a maximum sampling frequency of 125 Hz. Raw voltage values from each channel were buffered in system memory and written to disk in 20-s intervals using an SQLite-based routine. Timestamps were generated using the local system clock, and sequential buffer indexing was used to maintain consistent ordering of samples across write cycles.

A MATLAB App Designer interface was developed for experiment control, including configuration of sampling rate, output directory, and metadata fields. The OpenStride software interface is illustrated in Appendix A. Prior to each recording session, the interface triggers a Python-based zero-load calibration script to align baseline offsets across the four load cells. Real-time visualisation of the centre-of-mass (COM) position was provided by the Python acquisition program once recording commenced. Raw voltage signals were stored without acquisition-stage filtering to support analyses requiring unprocessed force traces, such as tremor quantification. A complete list of hardware and software resources required to reproduce the system is provided in Table 2.1, and a hardware schematic is shown in Fig. 2.1.

Category	Component / Software	Specification / Version	Source
Mechanical components	3D-printed walk plate (×1), plate holders (×4), base plate (×1), electronics-chamber lid (×1)	PLA, 20–40% infill	STL files (Supplementary)
	Acrylic enclosure	5-mm clear acrylic (35 × 45 cm), laser-cut	SVG file (Supplementary)
	Concrete ballast	35 × 35 × 5 cm	-
	Screws	M3.5 flat-head, 316/316L stainless steel, 8 mm length (×8)	-
		M3.5 flat-head, 316/316L stainless steel, 25 mm length (×8)	-
	Single-point load cells	Tedea Huntleigh Model 1004, 300 g capacity (×4)	Tedea-Huntleigh
	High-density EVA foam padding (×4)	≈100 kg/m ³ density, ~50 Shore A, 3 × 3 × 2 cm	-
DAQ card	PhidgetBridge DAQ card	PhidgetBridge 1046_0B	Phidgets Inc.
Electronics	USB connection	USB-A / USB-C	-
	Power	USB-powered system	-
	Host computer	Windows 10 / macOS	-
Computing hardware	Python	Python 3.10+	python.org
Firmware & acquisition	Phidget21 API	-	Phidgets Inc.
	Acquisition script	-	Supplementary
	MATLAB	R2024+	MathWorks
Software tools	MATLAB App Designer	R2024+	MathWorks
	SQLite	-	Python library
	Code repository	Acquisition, analysis, UI	(GitHub link)
Documentation	Assembly instructions	Mechanical + wiring schematics	Supplementary

Table 2.1. Key resources for the production of the OpenStride system

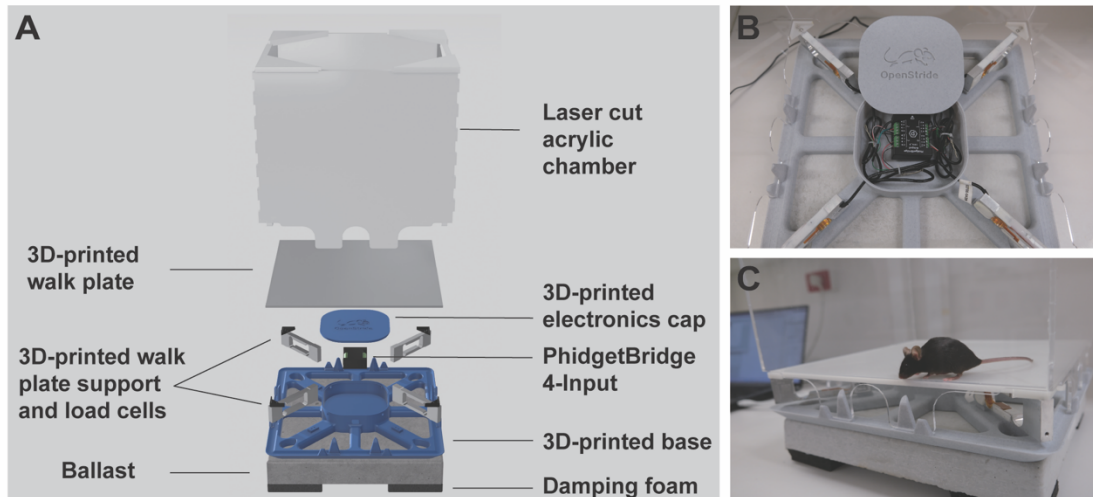


Figure 2.1: **A.** Primary components of OpenStride hardware. **B.** Assembled OpenStride without the walking plate and with the electronics lid removed. **C.** Fully assembled OpenStride system with a C57BL/6 mouse for scale.

2.3.3 Mechanical stability validation

The mechanical stability of the OpenStride system was evaluated using a series of bench-top tests performed without animals, based on computed COM trajectories obtained during acquisition. For all tests, force signals were sampled at 125 Hz.

To characterise static drift, a 100 g calibration mass was placed at the centre of the walking surface, and recordings were acquired for 60 s at 125 Hz. COM time-series data $x(t)$ and $y(t)$ were segmented into fixed-length, non-overlapping windows (1 s; 125 samples per window). For each window, drift amplitude was calculated as the radial standard deviation of COM position, defined as follows: $D = \sqrt{\text{var}(x) + \text{var}(y)}$. For each trial, window-wise drift amplitudes were summarised to obtain a single drift metric per recording.

2.3.4 Positional accuracy validation

Distance measurement was assessed using a finger-tracing procedure performed on the walking surface. The effective working area of the walking platform was $30 \times 30 \text{ cm}^2$. During

each trial, a finger was placed at one corner of the platform and moved diagonally across to the opposite corner before returning to the starting point; a complete forward–return motion was defined as one trace. A total of 6 traces were collected. For each trace, the measured path length was computed as the cumulative distance across consecutive COM samples: $L = \sum_{i=1}^{N-1} \sqrt{(x_{i+1} - x_i)^2 + (y_{i+1} - y_i)^2}$. The theoretical straight-line distance between opposite corners of the $30 \times 30 \text{ cm}^2$ workspace was calculated as $\sqrt{30^2 + 30^2} \text{ cm} = 44.3 \text{ cm}$.

2.3.5 Locomotor behaviour based on trajectories

Spontaneous locomotor activity was recorded by placing each animal individually into the hardware chamber for a 10-min session. Animals were allowed to freely explore the $30 \times 30 \text{ cm}^2$ arena without external stimuli. Force signals were sampled at 125 Hz and converted to real-time COM coordinates during acquisition. For analysis, COM trajectories $(x(t), y(t))$ were smoothed using a 15-sample moving-average filter.

Several COM-based metrics were extracted from the 10-min recordings. Path length was calculated as the cumulative Euclidean distance between successive COM samples: $L = \sum_{i=1}^{N-1} \sqrt{(x_{i+1} - x_i)^2 + (y_{i+1} - y_i)^2}$. This yielded a time-resolved cumulative distance curve over the full session. Instantaneous speed was defined as the displacement between consecutive COM samples divided by the sampling interval: $s_i = \frac{\sqrt{(x_{i+1} - x_i)^2 + (y_{i+1} - y_i)^2}}{\Delta t}$.

Low-mobility bouts were identified when average speed fell below 0.5 cm/s for one second or longer. Cumulative low-mobility bout duration was computed as the sum of all time points meeting this criterion. These metrics enabled characterisation of locomotor trajectories, speed profiles, and low-mobility computations throughout the 10-min exploration period.

Times spent in the centre vs the margin were computed based on a defined central area. In this manuscript, the centre was defined as a square occupying the central 50% of the arena,

whilst the margin was defined as the remaining 50%. This threshold is modifiable in OpenStride, and notably, may require adjustment based on subject size, i.e. rats *vs* mice.

2.3.6 Ataxia and tremor quantification

Ataxia and tremor metrics were derived from COM trajectories and speed signals obtained during spontaneous locomotion sessions. Locomotor ataxia was quantified using an ataxia ratio computed over 1-s windows. COM trajectories $(x(t), y(t))$ were segmented into non-overlapping 1-s windows. For each window w , when net displacement exceeded a pre-set threshold (10 mm used herein), cumulative path length was computed as $L_w = \sum_{i=1}^{N_w-1} \sqrt{(x_{i+1} - x_i)^2 + (y_{i+1} - y_i)^2}$, where N_w is the number of samples in the window. Net displacement was defined as the Euclidean distance between the first and last COM coordinates of the window $D_w = \sqrt{(x_{N_w} - x_1)^2 + (y_{N_w} - y_1)^2}$. The ataxia ratio for each window was then calculated as $A_w = \frac{L_w}{D_w}$. This metric thus captures the relative irregularity in trajectory, with higher ratios reflecting greater deviation from straight-line motion. Ataxia ratios were computed for all windows across each animal's recording.

Tremor quantification was based on speed fluctuations derived from COM trajectories. Speed was obtained as $s_i = ((x_{i+1} - x_i)^2 + (y_{i+1} - y_i)^2)/\Delta t$, where $\Delta t=8$ ms is the sampling interval when sampling at 125 Hz. The speed time series was detrended and segmented into 2-s windows with 50% overlap. Power spectral density (PSD) estimates were computed using Welch's method with a Hanning window. Tremor amplitude was defined as the integrated spectral power within a specified band (3–8 Hz used here): $P_{\text{tremor}} = \int_3^8 \text{PSD}(f)df$. To normalise tremor magnitude across animals and trials, the tremor score was calculated as the

ratio of the tremor band to the total power in the 0–20 Hz band: $T = \frac{\int_3^8 \text{PSD}(f)df}{\int_0^{20} \text{PSD}(f)df}$. This yielded a dimensionless tremor index for each recording.

Ataxia ratios and tremor scores were computed from recordings obtained from wild-type and *shaker* rats under identical conditions. For each animal, metrics were averaged across all valid 10-min locomotor sessions. These values were used for statistical comparisons between genotypes in the results section.

2.3.7 Statistical analyses

Statistical analyses reported were performed within the MATLAB (MathWorks) environment. Comparisons between wild-type and *shaker* rats for ataxia and tremor metrics were conducted using one-tailed heteroscedastic two-sample (Welch) t-tests. Data are presented as mean \pm standard deviation (SD) or mean \pm standard error of the mean (SEM), with statistical significance defined as $p < 0.05$.

2.4 Results

2.4.1 Mechanical stability and accuracy of position and distance

We first evaluated the mechanical stability of the OpenStride system under static and perturbed conditions. We placed a 100 g mass at approximately the centre of the walking platform for 60 s and showed that the centre-of-mass (COM) positions remained tightly clustered, with drift amplitudes below 200 μm throughout the recording (Fig. 2.2A).

Positional accuracy was evaluated using trajectories recorded during diagonal finger-tracing movements. Each trace consisted of a forward movement from one corner of the $30 \times 30 \text{ cm}^2$ workspace to the opposite corner, followed by a return to the starting point. Across 20 diagonals, the recorded COM trajectories formed diagonal paths that extended across the length of the workspace (Fig. 2.2B). The trajectories from different repetitions followed similar spatial paths, with variations in both the x- and y-coordinates observable along the diagonals. For each trace, applying a convolutional window with a width of 10 samples, the cumulative measured distance increased approximately in step with the theoretical true distance (Fig. 2.2C).

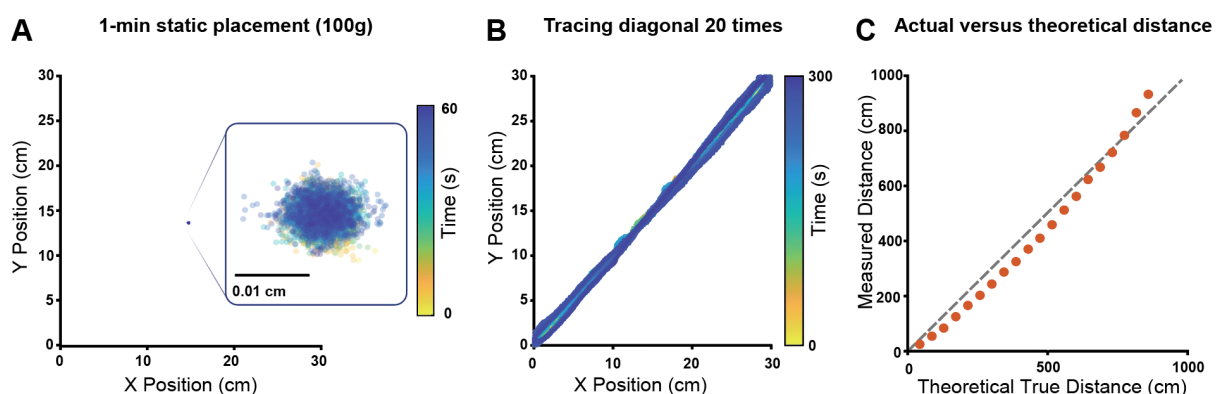


Figure 2.2: **A.** Centre-of-mass (COM) samples recorded over 60 s remain tightly clustered near the placement point. The spatial spread of COM positions indicates minimal drift during static loading. **B.** Trajectories recorded during 20 diagonal traces across the $30 \times 30 \text{ cm}^2$ workspace. Colours represent time within each trace. **C.** Cumulative measured distance (with a convolutional window of 10) plotted against the theoretical diagonal distance (dashed unity line).

2.4.2 Wild-type rodent locomotor validation

We evaluated locomotor behaviour using COM trajectories obtained during spontaneous exploration in both a wild-type C57BL/6 mouse and a wild-type Wistar Furth rat. Representative 5-min trajectories in the $30 \times 30 \text{ cm}^2$ arena are shown (Figs. 2.3A, 2.3D). The wildtype mice spent most of its time in the margin, while the wildtype rat spent similar time in the defined centre vs margin (Figs. 2.3B, 2.3E).

Cumulative distance, speed profile, and cumulative low mobility duration (with a 0.5 cm/s threshold applied) are shown for each 5-min session (Fig. 2.3C, 2.3F). Notably, the mouse ambulated more consistently than the rat during the 5-min recording duration, with only a single $\sim 2 \text{ s}$ low-mobility bout, resulting in substantially more distance travelled than the rat.

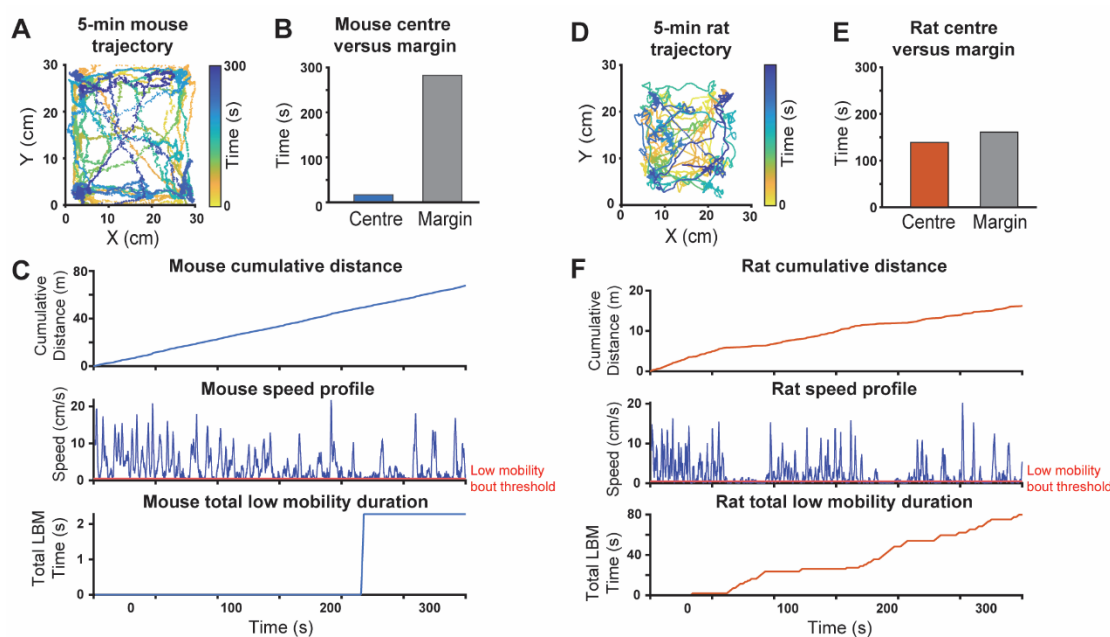


Figure 2.3: **A.** Trajectory from a 5-min mouse recording within the $30 \times 30 \text{ cm}^2$ workspace. **B.** The mouse spent most of its time in the margin rather than in the centre 50% of the arena. **C.** Cumulative distance, speed over time, and cumulative low mobility duration are shown from the same recording, with only one short period of low-mobility bout recorded. **D-F.** A 5-min rat recording is shown as in A-C. Notably, the rat travelled considerably less distance and had substantially more low mobility duration.

2.4.3 Tremor and ataxia measurements

Finally, we examined COM-derived ataxia and tremor metrics in wild-type Wistar Furth (n=6) and Wistar Furth *shaker* (n=6) rats. Representative 1-s trajectory segments showed a broad range of ataxia ratios, with higher ratios corresponding to increasingly irregular paths (Fig. 2.4A). Across animals, *shaker* rats displayed higher ataxia ratios than wild-type controls (Fig. 2.4B). Individual data points show non-overlapping distributions across groups, and group means differed significantly ($p = 0.000137$). Power spectral density (PSD) estimates of COM-derived speed revealed clear group differences (Fig. 2.4C). Wild-type rats showed smoothly decaying broadband spectra, whereas *shaker* rats exhibited increased power within the 3–8 Hz range. This difference was quantified using a normalised tremor score, which was higher in *shaker* rats than in wild-type rats (Fig. 2.4D; $p = 0.000753$).

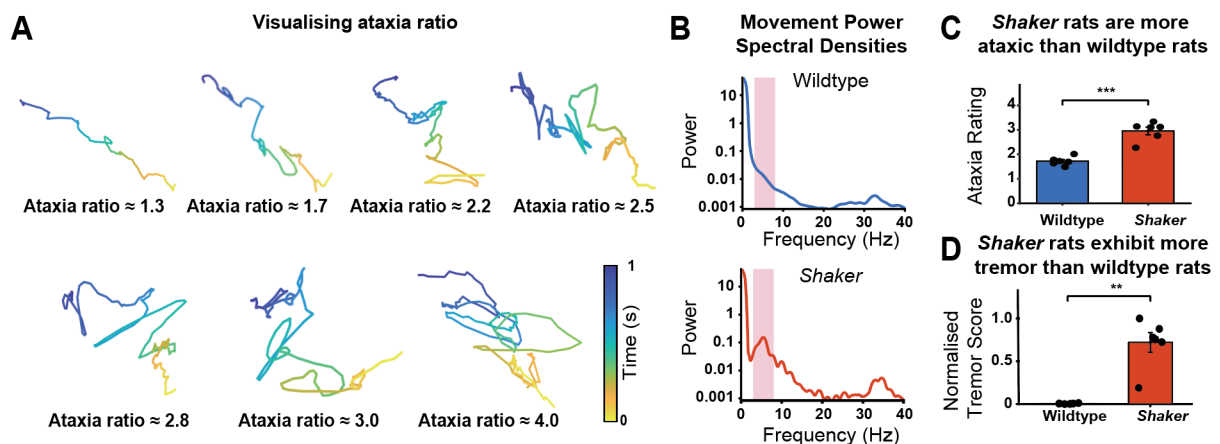


Figure 2.4: **A.** Example 1-s trajectory segments illustrating ataxia ratios ranging from approximately 1.3 to 4.0. **B.** Speed PSD estimates for representative wild-type (above) and *shaker* (below) rats. Wild-type spectra show broadband decay to 20 Hz without clear peaks, whereas *shaker* spectra display elevated power in the 3–8 Hz range (pink shaded region); **C.** Ataxia ratios for individual wild-type (n = 6) and *shaker* rats (n = 6). Data points represent per-animal means; bars show group means \pm SEM. *Shaker* rats exhibited higher ataxia ratios than wild-type controls ($p = 0.000137$). **D.** Normalised tremor scores (ratio of 3–8 Hz power to total 0–20 Hz power) for wild-type and *shaker* rats. Individual points indicate per-animal values; bars show group means \pm SEM. *Shaker* rats exhibit higher tremor scores than wild-type controls ($p = 0.000753$).

2.5 Discussion

In this work, we developed an open-source, low-cost force plate actometer called OpenStride, including both software and easily manufactured hardware. Currently, we have enabled OpenStride to quantify several aspects of gait and movement. Specifically, through centre-of-mass tracking in naturalistic behaviour, OpenStride quantifies speed, distance, bouts of low mobility, tremor, ataxia, and centre-*vs*-margin comparisons. The hardware described has been designed to be produced in any setting with access to a standard large-format 3D printer and a laser cutter, including academic fabrication laboratories, public libraries, and community maker spaces or developer hubs that support DIY technologies.. At the time of publication, the total cost of manufacturing this force plate actometer is approximately \$800 AUD, assuming the user already has access to a standard computer and the aforementioned manufacturing resources. Given the open-source nature of this design, we have detailed the impact of several variables on system outcomes, and it is our intent that end users will be able to make informed decisions on how to utilise this system in a way that reflects their specific needs.

OpenStride builds off of Fowler et al.'s initial design (Fowler et al., 2001); we have previously coupled this hardware with our own custom software to quantify ataxia (Anderson et al., 2019; Anderson et al., 2025; Figueroa et al., 2023; Kuo et al., 2019; Lang et al., 2020), self-grooming behaviours (Anderson et al., 2024), and open-field assessments (Scoles 2022, bioRxiv). It was also designed to remain compatible with the above-mentioned and similar experimental paradigms, supporting quantitative analyses in studies such as pharmacological locomotor assessments (Fowler et al., 2010), investigations of dietary or developmental effects on motor activity (Levant et al., 2011; Levant et al., 2010), models of sensorimotor gating and neuropsychiatric behaviour (Godar et al., 2016), transgenic and neuroinflammatory models (Hein et al., 2012; McCarson et al., 2019), as summarised by Zarccone (Zarccone, 2022).

Several software and hardware considerations should be noted. First, while we have previously designed methods for FPA-based self-grooming quantification, we have not enabled these for OpenStride. Given that previous grooming-focussed work was carried out solely in the context of C57Bl/6 mice and dependent on machine learning-based classifiers, our enabling of this feature in OpenStride would depend on training the classifier in the context of a broader variety of models. Further, to enable this for rats, a second classifier would need to be generated and trained on several distinct rat strains for greater utility. However, given that the system saves raw data, it would be possible to design new analyses in the future and apply them to previously collected data.

Second, we note that signal-to-noise ratios will remain inferior to prior FPA designs. Original Fowler-designed FPA systems utilised higher-end Honeywell load cells (Model 31 060-1435-01) at a cost of \$6000 AUD for the system at last time of sale, yielding higher-fidelity centre-of-mass recordings. Notably, given the 3D-printed nature of the OpenStride baseplate, accommodating for different sensors would be possible with moderate effort if needed. With the current OpenStride design, wild-type rat ataxia ratios averaged about 1.8, compared to ~1.6 using an identical calculation on an original Fowler-built FPA (Anderson et al., 2019; Figueroa et al., 2023), showing the slightly higher signal-to-noise ratio of the original Fowler system.

Third, static drift characterisation was performed under fixed conditions. The influence of subject weight across the range typical of mice and rats (approximately 20–500 g) and extended recording durations (e.g., several hours) on drift magnitude remains to be systematically evaluated. Users could therefore consider performing local drift validation under their specific experimental conditions prior to data collection.

Fourth, it should be noted that both mice and rats were assessed using the same chamber dimensions. Given the substantial difference in body size between species, the relative size of the measurement area differs considerably, which may influence behavioural metrics in a

species-dependent manner. In particular, centre-vs-margin time, cumulative distance, and low mobility bouts may not be directly comparable across species, as rats occupy a proportionally larger portion of the chamber than mice. Consistent with this, x-y centre-of-mass trajectories suggest that rats do not approach chamber walls as closely as mice, which may reflect spatial constraints rather than true differences in thigmotactic behaviour. Future implementations may benefit from scaling chamber dimensions to reflect the relative body size of the species under study.

Fifth, we note that temporal resolution is lower with OpenStride than with our previously reported FPA work. Previously, we interfaced load cells from Fowler FPA systems to computers using National Instruments (NI) data acquisition (DAQ) cards, with which we regularly collected centre-of-mass data at 1000 Hz. Our chosen PhidgetBridge system collects data at a maximum rate of 125 Hz, which is sufficient for most potential applications. However, modifications may be possible to enable the use of NI DAQ cards or other high-temporal-resolution input devices. Finally, OpenStride currently supports Mac and Windows operating systems. Should the system see broader adoption, future development may extend compatibility to other operating systems,.

OpenStride has been designed as an open-source, low-cost, and easily manufactured force plate actometry system. While OpenStride is currently capable of quantifying speed, distance, bouts of low mobility, tremor, ataxia, and centre-vs-margin comparisons, it is the intent of the authors that further capabilities will be added in the future. Given the open-source nature, numerous modifications to both hardware and software are possible, with the goal of flexibility to suit user needs. To date, force plate actometry has been used modestly in neuroscience research, with several hundred uses reported to date (Zarcone, 2022). Given a need for more naturalistic behavioural and motor quantification in numerous contexts (Cisek

et al., 2024; McCullough et al., 2021), OpenStride may serve to enable a greater uptake of force plate actometry.

3.1 Abstract

Introduction: In Chapter 2, we demonstrated that the OpenStride system provides the capability to quantify locomotor activity, tremor, and ataxia in rodents. However, it remained important to determine how to optimise system configuration. Understanding whether and how factors such as subject mass, platform mass, load cell excitation voltage, mechanical damping, and signal processing affect system performance is essential for optimising deployment across diverse experimental contexts and rodent species.

Methods: We evaluated the influence of key design parameters on OpenStride’s measurement stability and signal quality. First, static drift and susceptibility to external mechanical perturbation were quantified under varying loads. Next, the effects of platform mass, load cell excitation voltage, and mechanical damping on stability were evaluated. Finally, signal processing approaches, including temporal smoothing and filtering methods, were assessed to characterise their impact on noise reduction and trajectory fidelity.

Results: System stability improved with increasing applied load, and external perturbation effects were similarly attenuated by increased load, suggesting that heavier rodent subjects may yield better-quality recordings. Load cell excitation voltage influenced measurement accuracy, with higher voltages (up to the manufacturer-specified maximum of 15 V) producing distance measurements closer to theoretical values. Mechanical damping was found to significantly reduce perturbation susceptibility, with foam thicknesses of 2 cm or greater producing markedly lower response to external perturbation. Walking platform mass had limited impact on performance within the tested range (200–500 g), although a 200 g platform appeared suboptimal for mouse recordings. Several forms of signal filtering reduced noise-induced path length overestimation, with combined low-pass and moving-average filtering performing robustly across a range of parameter settings.

Conclusions: OpenStride performance can be optimised through informed selection of hardware and signal processing parameters. The systematic characterisation presented here defines the operating ranges and trade-offs that allow users to balance measurement sensitivity, noise, and mechanical robustness across rodent species and experimental paradigms.

3.2 Introduction

The baseline OpenStride system described in Chapter 2 demonstrated the capability to quantify locomotor activity, tremor, and ataxia in rodent models, achieving high positional accuracy and successful discrimination of motor phenotypes in proof-of-concept studies. However, measurement quality in force-based platforms is influenced by multiple interacting factors. While the original Fowler-designed FPA implementations utilised precision load cells and custom mechanical designs optimised through iterative refinement (Fowler et al., 2001), OpenStride's emphasis on accessibility and low cost necessitates a balancing of measurement fidelity with the constraints imposed by readily available components and standard fabrication methods.

Three primary considerations motivate system optimisation. First, the system is intended to support measurements across rodent species spanning a broad mass range, from ~20 g mice to ~500 g rats. As described in chapter 2, force transduction exhibits load-dependent signal-to-noise ratios, with lighter subjects generating smaller ground reaction forces, leading to reduced signal amplitudes relative to baseline sensor noise (Bobbert et al., 1990; Deacon et al., 2006; Fowler et al., 2001). Second, experimental environments can introduce mechanical perturbations, movement artifacts from nearby personnel, or vibrations from nearby equipment, all of which can compromise measurement stability, as also briefly described in chapter 2 (Brownjohn et al., 2004; Deacon et al., 2006; Middleton et al., 1999). Characterising the system's susceptibility to such disturbances and identifying design features that enhance

robustness will enable more reliable data collection in laboratory settings. Third, reducing baseline noise through hardware optimisation and signal processing refinement will improve trajectory precision, increase capability to detecting subtle motor phenotypes, and enhance reproducibility across recordings and laboratories (Button et al., 2013; Mathis et al., 2020).

Several design parameters are readily modifiable within OpenStride's open-source framework. Specifically, it is straightforward to modulate the platform mass, excitation voltage, mechanical damping and signal processing approaches, and characterising the effects of each on system performance is important in order to help end-users make informed decisions based on experimental requirements and subject characteristics. Thus, this chapter presents an evaluation of the above-stated design parameters, characterising their effects on OpenStride's measurement stability, noise characteristics, and trajectory accuracy through static and controlled perturbation tests, as well as with rodents. The findings provide practical guidance for users to configure OpenStride deployments that balance sensitivity, robustness, and measurement fidelity according to their experimental needs.

3.3 Methods

3.3.1 Animals

All procedures involving animals were approved by the University of Sydney Animal Ethics Committee (protocols 2023/AE002319 and 2024/AE002517) and performed in accordance with the Australian Code for the Care and Use of Animals for Scientific Purposes as well as the Animal Research Act 1985. In total, one adult mouse and one adult rat were utilised in this chapter. In both instances, rodents were housed 2-5 per cage under a standard 12:12 hour light cycle and given access to food and water *ad libitum*. The mouse utilised was of the C57BL/6 background, and the rat utilised was of the Wistar Furth background.

3.3.2 Load vs mechanical stability

To assess the effect of load magnitude on stability, the static drift protocol described in 2.3.3 was repeated with calibration masses of 0, 20, 50, 100, 200, 500, and 1000 g placed at the walking platform centre. For each load condition, three independent 30-min recordings were obtained. COM trajectories were processed as above, and drift amplitude D was computed for each window and summarised for each trial, providing a load–drift relationship across the tested mass range.

Susceptibility to external mechanical disturbance was assessed by dropping a 2.7 g ping-pong ball from a fixed height of 10 cm onto the benchtop exactly 10 cm from the edge of the force-plate base. Each trial consisted of a 10-s unloaded baseline recording followed by a ball impact occurring 5-s into the recording. The disturbance window was defined as the 2-s interval following the first ball–surface contact. Peak COM displacement during this window, relative to the mean COM position during the 2-s baseline period, was used to quantify the transient effect of the disturbance on system stability.

The disturbance protocol described above was repeated with additional static loads placed at the centre of the walking surface, with masses of 20, 50, 100, 200, 500, and 1000 g tested. For each load condition, five ball-drop trials were collected. For each trial, baseline COM position was taken from the 2-s period preceding impact, and transient disturbance response was quantified as the peak COM displacement within the 2-s post-impact interval. This procedure enabled assessment of how the load on the platform influenced the magnitude of transient disturbance effects.

3.3.3 Plate mass vs noise

The effect of platform mass on trajectory noise was assessed by fabricating walking plates with varying 3D print infill densities, yielding platform masses of 200g, 300g, 400g and

500g. All platforms maintained identical external dimensions ($30 \times 30 \times 0.5$ cm) and surface characteristics to ensure a consistent subject experience. For each platform mass condition, spontaneous locomotor recordings were obtained from a wild-type C57BL/6 mouse and a wild-type Wistar Furth rat during 10-min sessions. Ataxia ratios were computed as described in Section 2.3.6, serving as a proxy measure for trajectory noise under naturalistic movement conditions. Given that wild-type animals would be expected to exhibit consistent coordinated movement (Brooks et al., 2009), OpenStride should consistently yield low ataxia ratios in wild-type animals and increases from baseline would likely represent system noise. Thus, ataxia ratio distributions were compared across platform mass conditions for each species to determine whether platform mass might influence system noise.

3.3.4 Load cell voltage input vs noise

Load cell excitation voltage was systematically varied (5, 10, and 15 V) to evaluate how analogue signal amplitude influences trajectory-based distance estimation accuracy. These voltages span the manufacturer-specified operating range while avoiding the lower extreme where signal quality may be compromised and the upper extreme approaching maximum rated voltage (15 V).

For each voltage condition, ten independent trials were performed. Each trial consisted of the finger-tracing protocol described in Section 2.3.4, in which a finger was moved diagonally across the 30×30 cm² workspace from one corner to the opposite corner and back, yielding ten complete diagonal traversals per trial. The theoretical straight-line distance for each diagonal was $\sqrt{30^2 + 30^2}$ cm = 42.4. For each trial, the measured path length was computed as the cumulative Euclidean distance across all ten diagonals: $L = \sum_{i=1}^{N-1} \sqrt{(x_{i+1} - x_i)^2 + (y_{i+1} - y_i)^2}$. Distance fidelity was quantified as the ratio of total measured distance to total theoretical distance ($10 \times 42.4 = 424$ cm) for each trial. This

procedure yielded ten independent distance ratio measurements per voltage condition ($n = 10$ per group, 30 total measurements), enabling statistical comparison of measurement accuracy across excitation voltages.

3.3.5 Damping

The influence of mechanical damping on external perturbation susceptibility was evaluated by varying the thickness of EVA foam pads positioned beneath each platform corner. Damping configurations tested included 0, 20, 30, 40, and 50 mm foam thickness. For each damping condition, the ball-drop external perturbation protocol described in Section 3.3.2 was performed using a 276 g platform and 100 g static load positioned at the platform centre. A 2.7 g ping-pong ball was dropped from a height of 10 cm onto the benchtop at 10 cm from the force-plate base. Peak COM displacement during the 2-s post-impact window, relative to the mean COM position during the 2-s pre-impact baseline period, was quantified to assess perturbation attenuation as a function of damping thickness. For each damping configuration, five ball-drop trials were performed to characterise reproducibility of the perturbation response.

3.3.6 Effects of filtration on noise

To evaluate the effect of temporal smoothing on position, and therefore, distance, moving-average filters of varying window lengths (1–25 samples) were applied to the COM trajectories prior to distance estimation. For each smoothing condition, we quantified using the ratio between measured and theoretical distances. This procedure characterised how smoothing and sampling resolution influenced trajectory-based distance estimates across repeated diagonal traces.

In addition to moving-average smoothing, alternative temporal filtering approaches were evaluated using the same finger-tracing recordings (10 round trips; 20 diagonal traversals).

The COM trajectories were processed using five commonly applied filters: median filtering, Gaussian smoothing, Savitzky–Golay filtering (Savitzky et al., 1964), Butterworth low-pass filtering (Butterworth, 1930), and exponential moving average (EMA) filtering. For each filter type, a single defining parameter was systematically varied to modulate smoothing strength: window size for moving-average, median, and Savitzky–Golay filters; Gaussian kernel width (σ) for Gaussian smoothing; cutoff frequency for Butterworth filtering; and smoothing factor (α) for EMA.

To assess potential interactions between filtering approaches, combined filtering configurations were examined. In the first condition, a Butterworth low-pass filter with a fixed cutoff frequency (25 Hz) was applied prior to moving-average smoothing, and the moving-average window size was varied (1–25 samples). In the other condition, the moving-average window was fixed (5 samples) and the Butterworth low-pass cutoff frequency was varied (1–25 Hz). For each parameter setting, filtered trajectories were segmented into 20 diagonal traversals, and distance accuracy was quantified as the ratio between measured and theoretical distance.

3.3.7 Statistical analyses

All statistical analyses were performed in MATLAB (R2024a, MathWorks, Natick, MA, USA). Data are presented as mean \pm standard error of the mean (SEM) unless otherwise specified. Statistical significance was defined as $p < 0.05$ for all tests. Sample sizes for each analysis are reported in the corresponding Results sections.

Pearson product-moment correlation coefficients were computed to quantify linear relationships between continuous variables, with correlation strength assessed using the coefficient of determination (r^2). This approach was used to evaluate load-dependent effects on static drift amplitude and perturbation-induced displacement (Section 3.4.1), linear trends

across platform mass conditions (Section 3.4.2), and the relationship between excitation voltage and distance measurement accuracy (Section 3.4.3).

One-way analysis of variance (ANOVA) was used to compare group means across categorical conditions. This was applied to ataxia ratios across platform mass conditions in mice and rats (Section 3.4.2), and to distance measurement accuracy across excitation voltage settings (Section 3.4.3), and to peak displacement across foam damping thickness conditions (Section 3.4.4). Degrees of freedom are reported as $F(df_between, df_within)$, where $df_between = \text{number of groups} - 1$ and $df_within = \text{total observations} - \text{number of groups}$. When ANOVA indicated a significant effect, post-hoc pairwise comparisons were conducted using Tukey's Honest Significant Difference (HSD) test to control family-wise error rate.

Descriptive analysis was used to characterise the relationship between filter parameters and measured-to-theoretical distance ratios across all filtering conditions (Section 3.4.5).

3.4 Results

3.4.1 Load-Dependent Stability

We quantified how measurement stability varied as a function of applied load using static drift and perturbation response protocols. Under static loading conditions, drift amplitude decreased monotonically with increasing mass across the tested range (0–1000 g; Fig. 3.1A). A significant negative correlation was observed between applied load and drift amplitude ($r = -0.499$, $n = 1,045,069$ samples, $p < 10^{-10}$), indicating that heavier loads consistently yielded more stable COM position estimates, although even low masses yielded an acceptable degree of drift in the context of most potential system uses.

To assess system robustness to external perturbations – representing minor bumps of the system surroundings or the presence of nearby equipment inducing a small degree of mechanical noise – we subjected the platform to controlled mechanical disturbances by

dropping a 2.7 g ping-pong ball from a height of 10 cm onto the benchtop at 10 cm from the device base. Under unloaded conditions (0 g), the impact produced clear, transient displacements in both x and y COM trajectories (Fig. 3.1B). Peak displacement amplitude during the 2-s post-impact window decreased significantly as a function of applied load (Fig. 3.1C). A significant negative correlation was observed between load mass and perturbation-induced displacement ($r = -0.370$, $n = 7000$ trials, $p < 10^{-10}$), demonstrating that increased platform loading attenuated mechanical sensitivity. Peak displacement decreased from approximately 6 mm at 0 g to below 2 mm at 1000 g, representing a greater than 3-fold reduction in perturbation susceptibility. These findings indicate that measurement stability improves with subject mass, with both static drift and dynamic perturbation response exhibiting load-dependent attenuation. However, again, even low masses yielded an acceptable response to minor external perturbation.

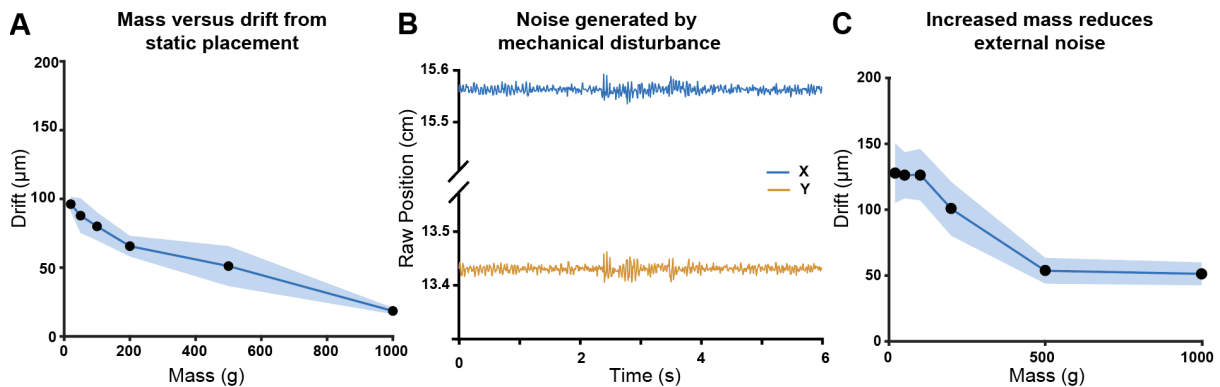


Figure 3.1: **A.** Static COM drift as a function of applied mass at the centre of the platform. **B.** Example x and y COM traces during a ping-pong-ball impact applied 10 cm from the platform. **C.** Bump-triggered COM drift as a function of applied mass, showing reduced mechanical sensitivity with increasing load. Data are mean \pm SD.

3.4.2 Platform Mass Effect

We evaluated whether platform mass influenced trajectory noise by fabricating walking plates with varying infill densities (200, 300, 400, 500 g) while maintaining identical external dimensions. Ataxia ratios were computed from 10-min spontaneous locomotor recordings in

wild-type animals, and we used this a proxy to interpret noise, as decreased signal to noise ratios would yield increased ataxia ratios in the same subject.

In wild-type mice, when utilising an optimised filtration method (described below in 3.4.5), mean ataxia ratios varied across platform masses: 1.64 ± 0.04 (200 g), 1.50 ± 0.03 (300 g), 1.52 ± 0.04 (400 g), and 1.53 ± 0.04 (500 g; Fig. 3.2A). One-way ANOVA revealed a significant effect of platform mass ($F(3,349) = 3.35$, $p = 0.019$). Post-hoc Tukey HSD analysis identified a significant reduction in ataxia ratio at 300 g compared to 200 g (mean difference = 0.14, 95% CI [0.004, 0.277], $p = 0.040$), representing an 8.5% decrease. No other pairwise comparisons reached statistical significance (all $p > 0.05$). Linear correlation analysis revealed only a weak negative relationship ($r = -0.079$, $p = 0.024$). Thus, a 200 g mass plate may be too light to optimise performance in the context of mouse experiments, but increasing beyond 300 g does not appear to improve performance. In wild-type rats, mean ataxia ratios were as follows: 1.51 ± 0.06 (200 g), 1.61 ± 0.05 (300 g), 1.39 ± 0.04 (400 g), and 1.42 ± 0.06 (500 g; Fig. 3.2B). One-way ANOVA revealed a significant effect of platform mass ($F(3, 812) = 3.48$, $p = 0.016$). Post-hoc Tukey HSD analysis showed that the 400 g condition yielded significantly lower ataxia ratios than the 300 g condition (mean difference = 0.22, 95% CI [0.033, 0.399], $p = 0.013$), representing a 13.4% reduction. However, no other pairwise comparisons were significant (all $p > 0.05$). Linear correlation trended towards significance ($r = -0.104$, $p = 0.051$), but given the minimal r value, it is reasonable to conclude that platform mass is not substantially important to system performance in an adult rat, so long as the platform is sufficiently rigid. Thus, in order to avoid overloading sensors, 200 g platforms may be most appropriate for use in adult rats, particularly large ones. Indeed, regardless of species, the practical impact of platform mass on measurement quality is limited within the tested range, and all tested masses within the 200–500 g range yield acceptable performance for both species.

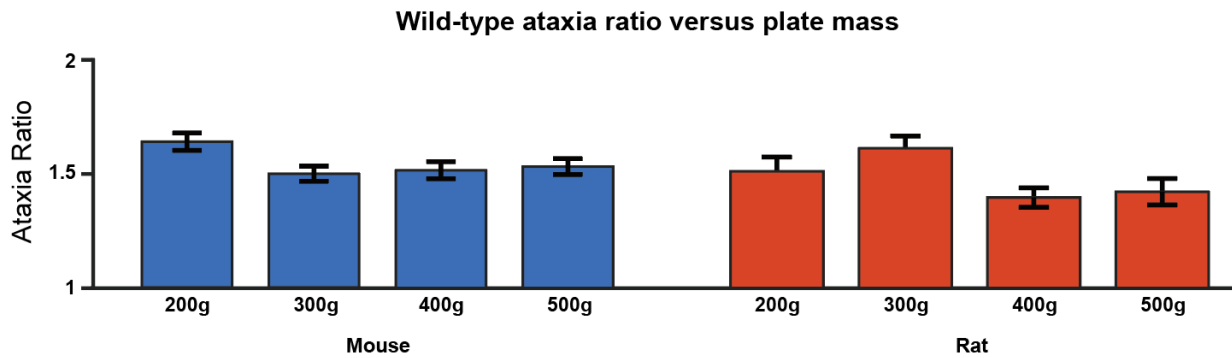


Figure 3.2: Ataxia ratio measured at different plate masses in (A) a wild-type mouse and (B) a wild-type rat.

3.4.3 Load Cell Excitation Voltage

We evaluated the influence of load cell excitation voltage on distance measurement accuracy across three voltage settings (5, 10, 15 V) spanning the manufacturer-specified operating range. Mean measured-to-theoretical distance ratios decreased systematically with increasing voltage: 1.097 ± 0.014 (5 V), 1.038 ± 0.011 (10 V), and 0.946 ± 0.006 (15 V; Fig. 3.3). One-way ANOVA revealed a highly significant effect of excitation voltage ($F(2,27) = 53.2$, $p < 0.001$). Post-hoc Tukey HSD pairwise comparisons revealed significant differences between all voltage pairs: 5 V versus 10 V (mean difference = 0.059, 95% CI [0.022, 0.096], $p = 0.0013$), 5 V versus 15 V (mean difference = 0.151, 95% CI [0.115, 0.188], $p = 2.6 \times 10^{-10}$), and 10 V versus 15 V (mean difference = 0.092, 95% CI [0.056, 0.129], $p = 3.3 \times 10^{-6}$). Correlation-based analysis demonstrated a strong negative relationship between voltage and distance ratio (Pearson's $r = -0.886$, $p = 7.5 \times 10^{-11}$; Fig. 3.3). Based on $r = -0.886$, excitation voltage accounted for 78.5% of variance in distance measurement.

The systematic decrease in measured-to-theoretical distance ratio with increasing excitation voltage indicates that higher voltages improve trajectory fidelity by reducing noise-induced path overestimation. At the manufacturer's maximum recommended voltage (15 V), distance measurements approached theoretical values with high accuracy (ratio = 0.946 ± 0.006). Notably, while a value of less than 1.0 may seem too low, we interpret this as achieving

straight traces but with the finger regularly not fully reaching the centre point over the load cell in either corner; thus, performance is likely best with a 15 V input. In contrast, the PhidgetBridge default voltage (5 V, consistent with standard USB voltage output) yielded a small degree of overestimation. These findings demonstrate that excitation voltage is an important parameter for optimising measurement accuracy, with higher voltages (≥ 10 V) recommended when maximum precision is required.

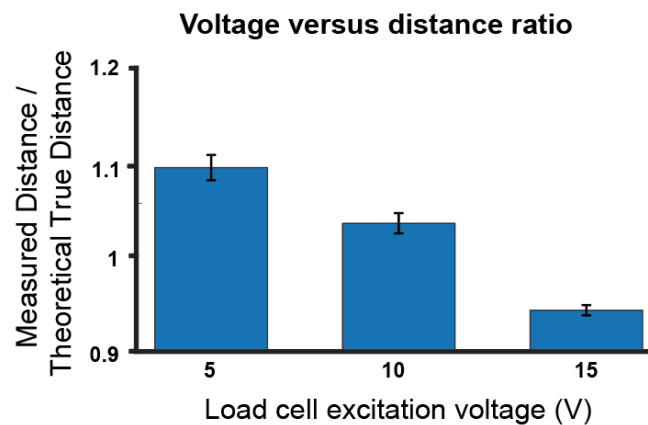


Figure 3.3: Measured-to-theoretical distance ratio vs load-cell excitation voltage. Increased voltage, up to the maximum input of 15 V significantly decreased distance ratio, suggesting improved signal-to-noise ratio.

3.4.4 Mechanical Damping

We investigated the influence of mechanical damping on perturbation susceptibility by varying EVA foam pad thickness (0, 10, 20, 30, 40, 50 mm) beneath the platform supports. Using a 276 g platform with 100 g static load, controlled perturbations were applied via the ping-pong ball drop protocol (Section 3.3.2). Peak COM displacement during the 2-s post-impact window was quantified for each damping condition (Fig. 3.4).

A total of 6 ball drop observations were analysed across the six foam thickness conditions. A one-way ANOVA confirmed a statistically significant effect of foam thickness on peak displacement ($F(5, 9076) = 34.37$, $p = 6.41 \times 10^{-35}$). Post-hoc comparisons using Tukey's HSD revealed that all conditions from 2 to 5 cm were each significantly better than both the 0 cm and 1 cm conditions (all $p < 10^{-10}$). Within the 2–5 cm range, 3 cm ($p = 0.013$)

and 5 cm ($p = 0.00029$) yielded decreased displacement than 2 cm, though the absolute differences were modest. Thus, 2 cm of damping foam damping is likely helpful in many use cases, with modest potential benefit from increasing further in contexts demanding particularly high precision.

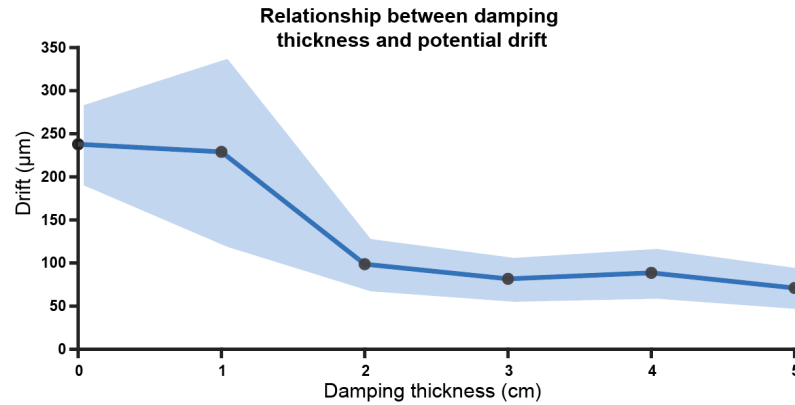


Figure 3.4: Bump-triggered centre-of-mass (COM) drift as a function of damping thickness, measured using a 276 g plate with a 100 g load.

3.4.5 Signal Processing and Filtering

Using the finger-tracing experiment previously used in Figures 2.2B and 3B, we first examined how simple convolutional smoothing influenced apparent trajectory length. Increasing the moving-average window from 1 to ~5 samples caused a step reduction in the ratio of measured to theoretical distance. Further increases beyond ~5–10 samples produced diminishing returns, quickly approaching 1.0 (Fig. 3.5A).

Applying alternative filtering strategies produced a similar overall pattern, but with filter-specific convergence profiles (Fig. 3.5B–F). Median filtering reduced the distance inflation more rapidly than the moving average, although larger windows were required before full convergence to the theoretical value was achieved (Fig. 3.5B). Gaussian smoothing produced a smooth, monotonic decay in the distance ratio as kernel width σ increased, with near-unity values reached once σ exceeded approximately 1–2 samples (Fig. 3.5C).

Savitzky–Golay filtering showed an order-dependent reduction in distance inflation. Higher polynomial orders produced greater overestimation at small frame lengths, with convergence toward unity occurring only at larger window sizes (Fig. 3.5D). Low-pass Butterworth and exponential moving-average (EMA) filtering showed distinct but complementary behaviours. For the Butterworth filter, low cutoff frequencies (strong low-pass filtering) yielded measured-to-theoretical distance ratios close to unity, whereas increasing the cutoff frequency progressively increased distance inflation (Fig. 3.5E). EMA filtering exhibited a monotonic reduction in measured path length with increasing window size, with the ratio stabilising near unity at larger spans (Fig. 3.5F).

To evaluate whether sequential filtering altered these trends, combinations of low-pass and moving-average smoothing were additionally examined (Fig. 3.5G–H). When a 25 Hz low-pass filter was applied prior to moving-average smoothing, varying the moving-average window produced only modest additional reductions in the measured-to-theoretical distance ratio (Fig. 3.5G). Compared with moving-average filtering alone, the initial overestimation at small window sizes was attenuated, and the ratio approached unity with relatively small window increases. Conversely, when the moving-average window was fixed at 5 samples and the low-pass cutoff frequency was systematically varied, the distance ratio remained close to unity across a broad range of cutoff frequencies (Fig. 3.5H). Very low cutoff frequencies produced slight reductions in apparent path length, whereas increasing the cutoff frequency led to minor increases in distance inflation. However, the magnitude of these effects was substantially smaller than those observed when varying either filter independently.

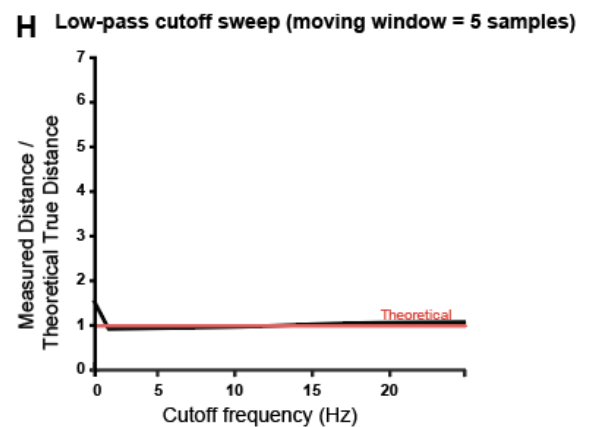
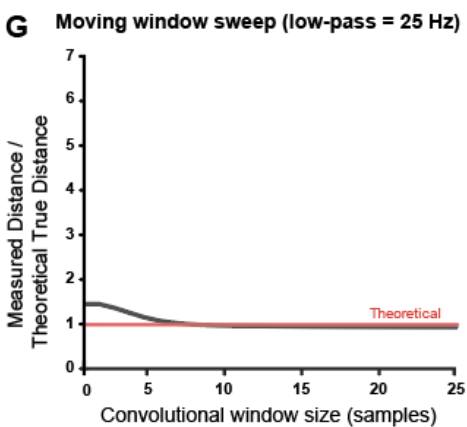
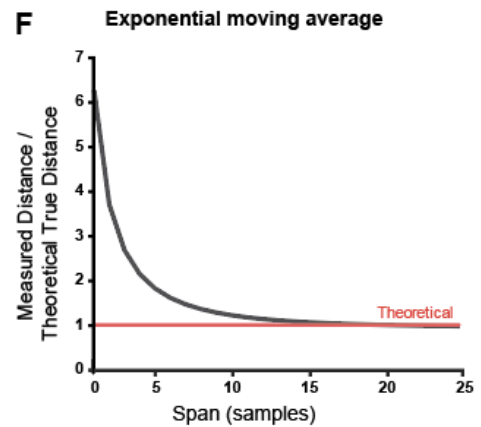
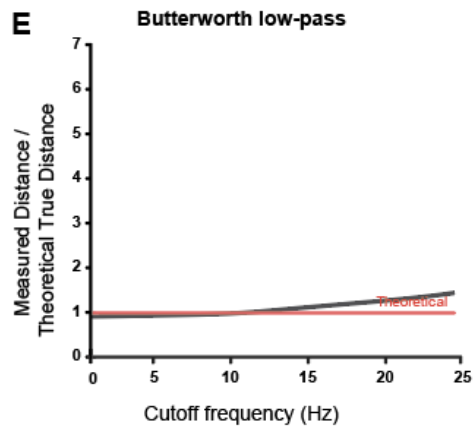
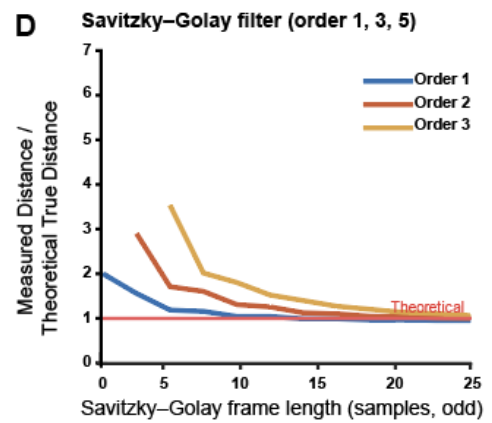
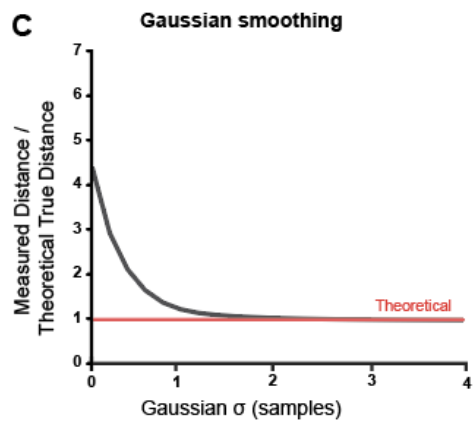
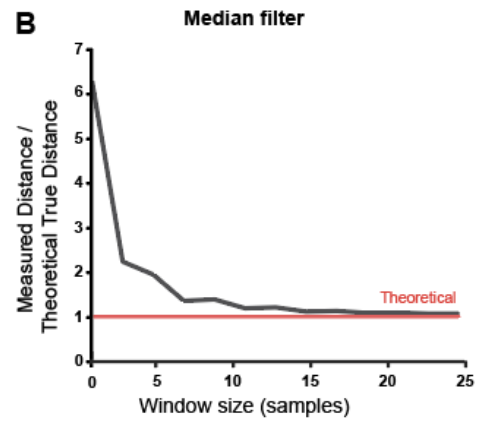
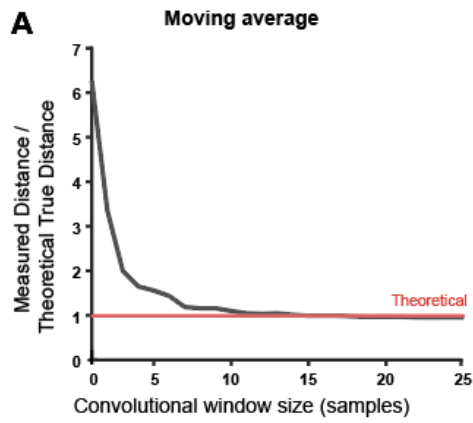


Figure 3.5: **A.** Effect of moving-average window size on the ratio of measured to theoretical distance. **B.** Effect of median-filter window size on the measured-to-theoretical distance ratio. **C.** Effect of Gaussian kernel width (σ) on the measured-to-theoretical distance ratio. **D.** Effect of Savitzky–Golay filter window size (polynomial order = 1,2,3) on the measured-to-theoretical distance ratio. **E.** Effect of Butterworth low-pass cutoff frequency on the measured-to-theoretical distance ratio. **F.** Effect of exponential moving average (EMA) equivalent window size on the measured-to-theoretical distance ratio. **G.** Effect of moving-average window size when combined with a fixed 25 Hz low-pass filter on the measured-to-theoretical distance ratio. **H.** Effect of Butterworth low-pass cutoff frequency when combined with a fixed 5-sample moving average on the measured-to-theoretical distance ratio.

3.5 Discussion

In this chapter, we reported on optimisation-focussed experiments using the OpenStride force plate actometry system first presented in chapter 2, finding that the modification of certain physical, electronic, or analytical approaches, or modified subject mass can alter the quality of system performance. Load cell excitation voltage exhibited a strong effect, with higher voltages systematically yielding less noise. Mechanical damping through the use of ~2 cm of EVA foam attenuated displacement in response to external perturbation, although additional damping yielded only modest further improvements. Signal processing approaches, including moving-average, median, Gaussian, Savitzky-Golay, Butterworth, and exponential moving average filters, converged to similar distance accuracy once sufficiently strong smoothing was applied, with window-based methods requiring approximately 5–10 samples for effective noise reduction while preserving trajectory fidelity. Finally, platform mass was tied to statistically significant but relatively modest effects on trajectory-derived noise metrics in wild-type mice and rats. In the context of mice, the use of a 300 g platform improved outcomes compared to a 200 g platform, although further mass increases didn't help. In the context of rats, no platform masses significantly improved upon outcomes collected with a 200 g platform; thus, using a minimal weight, maximally stiff platform is likely ideal in order to prevent sensory overload. Notably, in the original work on force plate actometry, a minimal mass, maximal stiffness platform is recommended (Fowler et al., 2001). Building on the chamber size limitations

identified in Chapter 2, these findings further support the case for developing species-specific platform dimensions. Scaling chamber size relative to animal body size may improve the fidelity of spatial behavioural metrics, particularly centre-vs-margin time and cumulative distance, and better capture thigmotactic behaviour that may currently be obscured by spatial constraints imposed by a uniform chamber size across species.

Further, system performance depends on subject mass. As anticipated, signal-to-noise ratios depend on the subject's mass, with heavier subjects resulting in reduced noise and reduced susceptibility to external perturbations. This fundamental relationship between applied load and measurement quality is characteristic of force transduction systems (Bobbert et al., 1990). OpenStride has been designed with the intention that it can be manufactured and assembled quickly at a low cost and will function as described herein in most contexts without modification. However, given the emphasis on accessibility and low cost, users intending to measure subtle changes, particularly in lightweight subjects such as mice or very young rats, may benefit from engaging with the open-source nature of OpenStride and considering alternative load cells with improved low-force sensitivity.

These findings have several practical implications for OpenStride usage and configuration. First, the strong load dependence of system stability (Fig. 3.1) indicates that users working with lightweight subjects (mice, juvenile rats) should anticipate higher baseline noise and may benefit from taking advantage of several modifications, including a moderate platform weight, reconfiguring load cell powering via a 15V external source, making use of damping, and careful exploration of filter options, perhaps combining a moving window with a low-pass filter. Conversely, users working primarily with adult rats can expect robust performance using the standard configuration so long as appropriate filtering approaches are used. However, if expanding software capabilities to identify or quantify subtle behaviours, the use of a 15V external source may be helpful, even for larger subjects.

Further, walking platform mass presents an important consideration for users to make. For mice, minimising the platform mass does not immediately appear helpful; notably, however, it is possible that platform stiffness in 3D-printed platforms is inferior to that of other construction methods, and it is possible that heavier platforms outperformed the lightest platform solely on the basis of improved stiffness. Thus, these findings cannot currently be extrapolated outside of 3D-printed walking platforms.

In the context of rats, further considerations need to be made in relation to platform mass that are dependent on the mass of the rat. With the sensors we have selected for OpenStride, each sensor has a mass rating of 300 grams. Notably, loading at 100-250% of the mass rating will lead to elastic overloading of the sensor, which may lead to temporary inaccuracy in measurements, while damage may occur with more than 250% of the recommended load. If using a 200 g platform, 50 g will be applied to each sensor without a subject. This may suggest, on its face, that measurement accuracy depends on keeping rats less than 250 g with a 50 g sensor. However, based on the size of the rat, it would not be physically possible in typical 4-legged posturing to place the centre of mass closer than ~4.5 cm from the corner. Applying a statics-based calculation, a rat greater than 350 g with a 200 g platform could yield an elastic overload condition. However, decreasing the platform mass to 40 g with alternate construction would enable a 400 g rat to be used with no elastic overload under static conditions. However, if using very heavy rats and needing very precise measurement, one may need to explore the use of larger mass rated sensors. Tedeo Huntleigh has produced a 600 g rated sensor in the same dimensions as the sensors reported on, enabling an easy swap, although at the time of this thesis, it is more difficult to acquire than the 300 g rated sensors we utilised. Finally, we note that as opposed to with static loading, dynamic loading due to ambulation, as well as rearing behaviours that place the centre of mass horizontally closer to the corner could induce elastic overloading at lower masses. All of this stated, in the context of our work, we

did not find evidence of significant problems generated by heavier mass subjects; however, if fine precision is required, users may need to investigate these details.

The selected Tedeo Huntleigh 1004 series load cells (300 g rating) represent a compromise between cost (~\$150 AUD per cell) and performance; higher-precision research-grade transducers (e.g., Honeywell Model 31 series, as used in original Fowler-designed systems) may offer superior signal-to-noise ratios but at substantially higher cost (~\$1500+ AUD per transducer). Notably, however, the use of sensors with alternate geometries would require modification to the platform base.

Beyond component selection, several methodological limitations warrant consideration. First, the parametric evaluations presented here examined individual design factors in relative isolation, without exhaustive exploration of all possible combinations or interaction effects. Interactive effects between platform mass, damping configuration, voltage settings, and signal processing parameters may exist but were not comprehensively characterised. For example, the optimal damping thickness may differ for lightweight versus heavyweight platforms, or the effectiveness of damping may depend on load cell sensitivity.

Second, the platform mass evaluation relied on ataxia ratio measurements in single wild-type animals (one mouse, one rat) rather than population-level assessments. While this approach enabled direct comparison across configurations within individual subjects, it precludes statistical evaluation of inter-animal variability and limits generalisability across animals of different ages, body compositions, or locomotor strategies (Crabbe et al., 1999). Biological variability in rodent motor behaviour is substantial even within inbred strains (Kafkafi et al., 2005), necessitating larger sample sizes for definitive conclusions regarding optimal hardware configurations across diverse experimental populations.

Third, the voltage and damping experiments were conducted using static loads and controlled perturbation protocols rather than biological subjects performing naturalistic

behaviours, in other words generating dynamic loads. While these approaches enabled systematic parameter manipulation and reproducible measurements (Deacon et al., 2006), they likely do not fully capture the complex, multi-frequency force dynamics generated during spontaneous rodent locomotion. Future validation using biological subjects across the tested parameter ranges would strengthen these findings.

Fourth, the filtering analysis focused exclusively on distance accuracy as the outcome metric. From the perspective of frequency-domain tremor quantification, preprocessing of raw trajectories with temporal smoothing is generally not recommended, as such filtering may attenuate or distort high-frequency components critical for tremor analysis (Fowler et al., 2001). Thus, in the context of tremor or other spectral analyses, filtering should not be used. The optimal filtering approach is therefore application-dependent: trajectory-based metrics (distance, velocity, spatial patterns) benefit from moderate smoothing to reduce noise, whereas frequency-domain analyses (tremor, oscillatory behaviours) require minimal preprocessing to preserve spectral content.

Finally, the current study did not assess long-term stability or material degradation effects. Viscoelastic materials such as EVA foam exhibit time-dependent mechanical properties including creep, stress relaxation, and compression set (Gibson et al., 1997), which may alter damping effectiveness over weeks to months of continuous loading, potentially requiring periodic replacement or recalibration. Similarly, 3D-printed PLA components may exhibit dimensional changes due to thermal cycling, humidity exposure, or mechanical stress (Farah et al., 2016), effects that were not characterised in the present short-term evaluation. Long-term stability studies spanning multiple months of continuous operation would be valuable for establishing maintenance schedules and replacement intervals for OpenStride deployments.

Based on the contents of this chapter, a preliminary user-specific optimisation strategy can be developed. Precise recommendations across parameters would depend on the subject species and mass, behaviours in question, and analytical specifics. Additional study would be beneficial; regardless, OpenStride users should be aware of the complex and interacting nature of system parameterisation. Furthermore, as OpenStride archives raw voltage output, users retain the flexibility to revisit collected data with alternative window sizes, revised algorithms, or emerging AI-based analytical approaches, enabling continued refinement without the need for repeated data collection.

Chapter 4: Conclusion and Future Work

4.1 Overall Summary

In this masters thesis, we sought to address the need for accessible, high-resolution motor and behavioural measurement in rodent models of neurological disorders by developing OpenStride, an open-source force plate actometry system. Through two aims, we established both the functional capabilities of the platform and systematically evaluating the effects of modulating key operating parameters, providing a starting point for users to select settings appropriate for their experimental needs.

In Aim 1, reported on in Chapter 2, we designed, fabricated, and validated the OpenStride system using readily commercially available components and standard fabrication methods, including 3D printing and laser cutting, ensuring that the system can be independently manufactured by laboratories worldwide. The system achieved positional accuracy within $\pm 200 \mu\text{m}$ across a $30 \times 30 \text{ cm}^2$ walk plate, maintained static drift below $200 \mu\text{m}$ during extended recordings, and successfully discriminated motor phenotypes between wild-type and *shaker* rats. Specifically, OpenStride quantified significant differences in both ataxia ratios and normalised tremor scores, demonstrating sensitivity to established motor phenotypes and enabling the characterisation of phenotype-specific behavioural signatures. Further, we demonstrated a capacity to collect clean recordings and quantify distance, velocity, and low mobility in both rats and mice.

In Aim 2 (Chapter 3), systematic parameter optimisation revealed that system performance depends on multiple interacting factors. Applied static load exhibited a significant effect on mechanical stability, with static drift and susceptibility to external perturbation reducing as load increased. Load cell excitation voltage emerged as an impactful tunable parameter, with signal noise reducing considerably with increased voltage input up to 15 V. Platform mass showed minimal but significant effects, although optimisation may be species

dependent, as discussed in 3.5. Further, mechanical damping reduced responses to external perturbation, and finally, several filtering methods provided additional optimisation useful for specific contexts.

Together, these findings establish OpenStride as a functional, cost-effective (~\$800 AUD) force plate actometry platform capable of quantifying locomotor activity, tremor, ataxia, and spatial behaviour in rodent models, with characterised operating ranges and reference information to support parameter selection for diverse experimental applications. It is our hope that in the future, a community of users collaborating together across laboratories and universities can repeat simple experiments to help create a data set across species, strains, and conditions, useful for well-powered open-source analytics.

4.2 Implications of the work

The development of OpenStride addresses a gap in the availability of force plate actometry systems. Since its introduction in 2001, FPA has demonstrated utility across diverse experimental contexts, with Fowler et al.'s original paper cited over 200 times across numerous applications (Zarcone, 2022), subsequent applications having spanned various areas, including neuropsychiatric disorders (Godar et al., 2016; Mosher et al., 2019; Mosher et al., 2018), movement disorders (Anderson et al., 2019; Figueroa et al., 2023; Kuo et al., 2019) and pharmacological studies (Fowler et al., 2010; Levant et al., 2011). Despite this demonstrated scientific value, adoption of FPA has remained modest, largely due to constraints in system availability and accessibility. The original systems developed by Fowler and colleagues utilised custom hardware, achieving both high signal-to-noise ratios and high sampling rates (Fowler et al., 2001), although these systems required substantial engineering expertise to construct and maintain. Commercial production was later undertaken by BASi Research Product as the Force Plate Actimeter®, which enabled turnkey deployment through integrated hardware–software

packages. However, these commercial systems introduced their own limitations, including fixed configurations, specific operation system, with purchasing prices of approximately \$15,000 AUD. Following the discontinuation of the Force Plate Actimeter®, laboratories were left with limited options: relying on aging legacy systems, undertaking custom redevelopment without standardised documentation, or abandoning the methodology altogether. This situation reflects a broader challenge in specialised behavioural instrumentation, where methodological continuity depends on the availability of niche hardware platforms. When commercial production ceases, access to established measurement techniques can be disrupted, creating persistent capability gaps.

OpenStride aims to address these barriers. Fabrication utilises methods increasingly standard in academic facilities, including 3D printing and laser cutting. The proliferation of maker spaces, fabrication labs, and additive manufacturing facilities in universities globally over the past decade (Beltagui et al., 2021; Bobic et al., 2025) has substantially reduced barriers to manufacture. Component sourcing is deliberately constrained to commercially available electronics (Tedea Huntleigh load cells, PhidgetBridge data acquisition interface) and standard hardware, minimising supply chain dependencies. Second, the total system cost of approximately \$800 AUD represents a substantial reduction, enabling deployment in resource-constrained settings and more easily facilitating high-throughput experimental designs where multiple systems may be operated in parallel. Third, cross-platform software compatibility (Windows and macOS) and modular code architecture support customisation and extension by researchers with varying computational backgrounds, promoting iterative refinement and community-driven development.

The availability of an open-source FPA platform may support broader integration of force plate actometry into neuroscience research. By reducing financial and technical barriers associated with proprietary systems, it provides an accessible approach for implementing high-

resolution motor behaviour measurements. This accessibility may be particularly relevant for translational research contexts, where reproducibility and consistency across experimental sites are important for validating behavioural phenotypes and therapeutic interventions. Furthermore, the open-source implementation enables full transparency of both hardware design and analytical methods, allowing independent verification and methodological refinement in line with current priorities in reproducible neuroscience (Button et al., 2013; Mathis et al., 2018; Pereira et al., 2022).

4.3 Comparison to other devices

The utility of OpenStride as a research tool depends on its capabilities and constraints relative to alternative measurement approaches. Compared to video-based tracking systems, OpenStride provides force-derived measurements that are insensitive to lighting conditions, visual occlusions, and contrast variations that can compromise optical tracking. The direct quantification of forces enables COM tracking without requiring visible body features, facilitating measurements during low-light conditions or within enclosed environments where camera placement is constrained. Additionally, the high temporal resolution of force signals (125 Hz) supports frequency-domain analyses for tremor quantification that would require high-speed videography to achieve comparable temporal precision. However, video-based approaches offer complementary advantages that OpenStride cannot replicate. Pose estimation methods such as with DeepLabCut (Mathis et al., 2018) and SLEAP (Pereira et al., 2022) provide kinematic information about individual limbs, body segments, and postural configurations, enabling analysis of motor coordination, and fine-grained limb trajectories that are inaccessible through COM measurements alone.

Compared to task-constrained motor assays such as the rotarod (Carter et al., 1999; Carter et al., 2001; Jones et al., 1968; Luong et al., 2011; Vandeputte et al., 2010), treadmill

(Brownjohn et al., 2004; Harnie et al., 2019; Herbin et al., 2007; Neckel et al., 2008; Wooley et al., 2005), elevated beam (Luong et al., 2011; Wheeler et al., 2021), and Erasmus ladder (Dijkhuizen et al., 2024; Namdar et al., 2020; Vinueza Veloz et al., 2012; Vinueza Veloz et al., 2015), OpenStride offers measurement in a naturalistic, open-field context that does not require training protocols or externally imposed motor tasks. This unconstrained assessment enables quantification of spontaneous exploratory behaviour, spatial preferences, and activity patterns alongside motor execution quality, providing insight into both motivational/affective states and motor control. The rotarod and elevated beam provide sensitive readouts of gross motor impairment but yield composite endpoint measures (latency to fall, number of foot slips) that do not capture the temporal dynamics or spectral characteristics of motor dysfunction. Similarly, while the Erasmus ladder offers detailed gait analysis with adaptive perturbations and substantially greater capabilities in the context of motor learning, the constrained linear path and task-specific demands may not reflect naturalistic movement strategies employed during spontaneous behaviour. OpenStride's primary limitation relative to specialised motor assays is the reduced ability to probe specific motor challenges or evoke motor responses. The rotarod explicitly tests balance and motor coordination under increasing challenge (Fowler, Zarcone, Vorontsova, et al., 2002; Hansen et al., 2013; Luong et al., 2011; Vandeputte et al., 2010), the Erasmus ladder assesses adaptive motor learning through obstacle perturbations (Namdar et al., 2020; Sathyanesan et al., 2019; Vinueza Veloz et al., 2012), and the elevated beam evaluates fine motor control under height-induced anxiety (Gardner et al., 2022; Wheeler et al., 2021). OpenStride, by contrast, quantifies motor performance during self-paced, unconstrained movement, which may be less sensitive under the condition of motor deficits that only manifest under challenging conditions.

Relative to existing FPA implementations, OpenStride sacrifices maximum sensor performance in favour of accessibility and cost. The original Fowler-designed systems utilised

load cells with superior low-force sensitivity. This difference reflects the trade-off between precision transducers (~\$1500 AUD per cell) (Fowler et al., 2001) and the lower-cost components (~\$150 AUD per cell) employed in OpenStride. As described in Chapter 3, digital filtering methods were applied to reduce noise and improve effective signal quality, enabling reliable extraction of behavioural data despite the lower intrinsic sensor sensitivity. For many applications, including locomotor activity quantification, gross tremor detection, and ataxia phenotyping in moderate-to-severe models, the performance of the baseline OpenStride configuration is adequate, as demonstrated by the clear discrimination of wild-type vs. *shaker* phenotypes (Chapter 2).

The comparisons presented above demonstrate that measurement assay selection involves multidimensional trade-offs rather than definitive superiority. OpenStride offers advantages in specific contexts (naturalistic behaviour, force-based metrics, continuous recording) while sacrificing capabilities provided by alternative approaches (detailed kinematics, controlled challenges, maximum signal precision).

4.4 Limitations

Beyond the comparative trade-offs discussed above, several limitations specific to our reported design and validation warrant consideration. First, as noted in Chapters 2 and 3, signal-to-noise ratios in force-based measurements are fundamentally load-dependent, with lighter subjects generating smaller ground reaction forces relative to baseline sensor noise. This constraint is shared across all force platform implementations but is particularly relevant for OpenStride given the use of moderate-precision load cells chosen as a compromise between cost and precision rather than for maximum precision. Users working with lightweight subjects (mice <20 g, juvenile rats) should anticipate elevated baseline noise and may benefit from load cell upgrades or alternative sensor configurations. The strong correlation between applied load

and drift amplitude and perturbation susceptibility documented in Chapter 3 provides quantitative guidance for predicting measurement quality across the rodent mass range.

Second, the system's reliance on a planar force-sensing surface constrains measurements to two-dimensional workspace and provides only indirect information about vertical behaviours such as rearing or jumping. While ground reaction forces contain signatures of vertical movements, such functionalities have not yet been made. Indeed, the current implementation prioritises simplicity and cost-effectiveness over three-dimensional measurement capabilities, accepting this constraint as appropriate for the target applications of locomotor activity, tremor, ataxia, and spatial exploration.

Third, the open-field, unconstrained measurement context enables naturalistic behavioural assessment but precludes controlled manipulation of specific motor challenges that can be evaluated with specialised apparatus. OpenStride cannot assess skilled reaching, precise paw placement on irregular surfaces, obstacle negotiation, or adaptive motor learning in response to perturbations, capabilities provided by paradigms such as the Erasmus ladder (Namdar et al., 2020; Vinueza Veloz et al., 2012), or ladder rung walking test (Metz et al., 2002). The platform is best suited for phenotypes that manifest during spontaneous, self-paced movement rather than those that emerge only during task-evoked motor responses.

Fourth, based on available resources at the time of this thesis, proof-of-concept testing in the context comparative motor phenotyping has only occurred in the context of a rat model. The system is clearly capable of measuring locomotion in a mouse. However, similar motor phenotyping studies in a mouse model of motor dysfunction would be helpful in the future.

Fifth, several methodological limitations in Aim 2 (Chapter 3) constrain generalisability. The platform mass evaluation relied on single wild-type animals (one mouse, one rat) rather than population-level assessments, precluding statistical evaluation of inter-animal variability and limiting conclusions about optimal configurations across diverse

experimental populations. Similarly, voltage and damping experiments employed static loads and controlled perturbation protocols rather than biological subjects or other dynamic loads, which may not fully capture the complex, multi-frequency force dynamics of spontaneous rodent locomotion. The parametric evaluations examined individual design factors in relative isolation without exhaustive exploration of interaction effects (e.g., whether optimal damping thickness depends on platform mass or load cell sensitivity), representing a practical constraint of the systematic optimisation approach.

Sixth, long-term stability and material degradation effects were not assessed in the present work. Perhaps most importantly, 3D-printed PLA components may deform slightly mechanical stress (Farah et al., 2016), and loss of mechanical alignment or loosening of parts could impact system performance. Establishing maintenance schedules, replacement intervals, and recalibration procedures for long-term deployments may represent an important direction for future validation work.

Finally, the open-source design introduces variability across implementations due to differences in component sourcing, manufacturing precision (e.g., 3D printer settings and calibration), and assembly procedures. In the context of manufacturing precision with a 3D printer, a great deal of parameters may need to be tuned, particularly for a novice user, to print all parts optimally. While documentation and assembly instructions mitigate this concern, achieving consistent performance across laboratories requires local validation protocols and calibration procedures. The finger-tracing and static drift tests described in Chapter 2 provide straightforward validation approaches that would be advisable be perform for each newly constructed system to verify positional accuracy and mechanical stability.

Collectively, these limitations define the boundaries within which OpenStride provides reliable measurement. The system is most appropriate for adult rodents (>30 g), two-dimensional trajectory analyses, spontaneous behavioural contexts, and applications where

moderate signal precision is acceptable. Users requiring maximum sensitivity in lightweight subjects, three-dimensional kinematic resolution, task-evoked motor responses, or long-term deployment without recalibration may need to consider adjustments, alternative approaches, or accept performance constraints. Importantly, many of these limitations may be addressable through hardware modifications (load cell upgrades, and alternate parameterisation), methodological extensions (population-level validation studies, longitudinal assessments), or procedural standardisation (calibration protocols, maintenance schedules), directions that represent opportunities for future development rather than fundamental barriers to utility.

4.5 Future Directions:

Several avenues for extending OpenStride's capabilities and broadening its applications merit consideration. First, expanding the analytical repertoire beyond the current metrics (distance, velocity, low-mobility bouts, centre-vs-margin time, ataxia ratio, tremor score) would increase OpenStride's utility across diverse experimental contexts. Prior FPA work has demonstrated machine learning-based classification of complex grooming behaviours (Anderson et al., 2024), and operant conditioning paradigms assessing response vigour and effort allocation (Zarcone et al., 2009). Implementing similar analytical approaches within the OpenStride software framework and validating their performance across rodent species and strains would extend the platform's applicability to neuropsychiatric models characterised by repetitive behaviours, motivational deficits, or altered exploration patterns.

Second, hardware modifications targeting specific experimental requirements represent promising customisation opportunities. For applications requiring maximum sensitivity in lightweight subjects, upgrading to higher-precision load cells or implementing amplification stages for signal conditioning could improve signal-to-noise ratios at the cost of increased component expense. For applications requiring higher temporal resolution, replacing the

PhidgetBridge interface with National Instruments or alternative data acquisition cards supporting kilohertz sampling rates would enable more detailed frequency-domain analyses. The modular design of OpenStride's hardware and software architecture supports such modifications without requiring complete system redesign.

Third, population-level validation across diverse rodent strains, ages, and disease models would strengthen confidence in the system's generalisability and establish normative ranges for key metrics. The present work validated OpenStride using C57BL/6 mice and Wistar Furth rats (wild-type and *shaker*), representing a limited sampling of the genetic and phenotypic diversity employed in neuroscience research. Systematic characterisation of locomotor patterns, ataxia ratios, and tremor profiles across commonly used inbred mouse strains (e.g., 129S1/SvImJ, FVB/NJ, BALB/cJ) and rat strains (e.g., Sprague-Dawley, Long-Evans, Lewis) would represent a great deal of work, but it could provide baseline reference data for interpreting experimental results and identifying strain-specific measurement considerations. Similarly, validation across developmental stages (juvenile, adult, aged) and established disease models (Parkinson's, Huntington's, cerebellar ataxias) would demonstrate sensitivity to known motor phenotypes and establish effect sizes for power analyses. To further support such efforts, routinely reporting a brief standardised FPA recording alongside primary experimental findings, such as the first five minutes of an animal's initial introduction to the platform, could facilitate future meta-analyses across species, strains, and laboratories.

Fourth, investigating potential applications beyond motor phenotyping may reveal additional utility for the FPA platform. Recent work has applied force-based measurements to assess anxiety-like behaviour through spatial exploration patterns (Godar et al., 2016) and operant behaviour through response force requirements (Zarcone et al., 2009). Exploring whether OpenStride can detect phenotypes in models of depression (quantification of lack of persistence if combined with a task), obsessive-compulsive disorder (repetitive behaviour

quantification), or ADHD (hyperactivity and impulsivity metrics) would expand the platform's relevance to neuropsychiatric research domains. However, such applications would require careful validation against established paradigms to ensure that force-derived metrics provide meaningful readouts of the target behavioural constructs.

Fifth, long-term reliability and maintenance requirements merit systematic evaluation. Conducting extended operation studies (e.g., daily recordings over 6-12 months) would characterise drift in mechanical alignment, force calibration, and component performance, establishing evidence-based recommendations for recalibration intervals (currently applied with every new recording session within our working group) and preventive maintenance. Similarly, evaluating the effects of component substitutions (e.g., alternative PLA filament suppliers, different EVA foam densities) on system performance would provide guidance for troubleshooting and adaptation to local component availability. Such practical considerations, while potentially less scientifically exciting than novel analytical methods or biological applications, are important for translating OpenStride from a proof-of-concept prototype to a reliable, widely adopted measurement tool.

Finally, the long-term viability of OpenStride as a community resource depends on sustained repository maintenance and version management. Open-source instrumentation requires ongoing effort: incorporating bug fixes, updating documentation for component availability changes, maintaining software compatibility, and implementing version control. Clear versioning conventions for hardware designs and software releases would support reproducibility and enable systematic comparison across studies. Sustainable maintenance may require institutional commitment or consortium arrangements rather than individual developer efforts alone. Without structured support, through dedicated positions, multi-laboratory collaborations, or integration into broader open-source initiatives, repositories risk abandonment as developers' transitions, recreating the accessibility barriers that motivated the

open-source approach. The present work establishes initial conditions through functional validation and public documentation, but realising broader impact depends on mechanisms for sustained community engagement that extend beyond this thesis.

Taken together, these further developments and validations would strengthen the OpenStride platform. Expanding the analytical framework, refining hardware configurations for specific experimental requirements, and validating performance across a broader range of animal models and experimental conditions would improve confidence in the system's applicability. In addition, systematic evaluation of long-term reliability, component variability, and maintenance requirements would support consistent operation over extended periods. Addressing these areas through incremental technical refinement and empirical validation would clarify the system's capabilities and limitations and support its effective use in behavioural neuroscience research.

4.6 Conclusions

This thesis established OpenStride as a functionally validated, accessible alternative to traditional force plate actometry systems, addressing the need for objective, high-resolution motor and behavioural measurement in rodent models of neurological disorders. Through design, fabrication, and validation (Aim 1), we demonstrated that a system constructed from readily available components and standard manufacturing processes can achieve acceptable measurement performance and successfully discriminate motor phenotypes between wild-type and ataxic rodents. Through parametric optimisation (Aim 2), we characterised the effects of key design parameters on system stability and measurement quality, providing quantitative guidance for users to configure OpenStride according to species, experimental priorities, and environmental conditions.

The core contributions of this work are as follows. First, the comprehensive hardware designs, software implementation, validation tests, and optimisation parameters reduce the technical barriers that have historically constrained FPA adoption, enabling laboratories worldwide to construct and deploy force plate actometry systems without highly specialised engineering resources or substantial financial investment. Second, the open-source framework supports community-driven development and iterative refinement, facilitating the incorporation of novel analytical approaches, hardware modifications, and application-specific customisations that reflect the evolving needs of the neuroscience research community. Third, the systematic characterisation of load-dependent stability, voltage-dependent accuracy, and species-specific platform mass effects provides generalisable insights into force-based measurement principles that, in some cases, may extend beyond the specific implementation described here, informing future force platform designs and optimisation strategies.

OpenStride is not intended as a universal replacement for existing behavioural measurement methods but rather as a complementary tool that occupies a distinct niche: quantitative, objective assessment of motor and behavioural phenotypes during naturalistic, unconstrained movement. For applications requiring detailed kinematic analysis, task-evoked motor responses, or specific motor challenges, integration with video-based tracking systems or specialised motor assays remains appropriate. However, for phenotypes that manifest during spontaneous locomotion, including activity levels, spatial exploration, tremor, ataxia, and repetitive behaviours, OpenStride provides continuous, multi-dimensional measurement within a unified recording session, supporting comprehensive behavioural characterisation with minimal experimenter intervention.

The ultimate impact of OpenStride will depend on adoption by the research community and the extent to which open-source collaboration drives iterative improvements in hardware, software, and analytical methods. By releasing all documentation, design files, and source code

through public repositories at the time of manuscript publication, we aim to catalyse a community of practice around accessible force plate actometry, enabling researchers to contribute enhancements, share validation datasets, and collectively address limitations identified in early implementations (Pearce, 2012; Pereira et al., 2022).

In conclusion, OpenStride provides a valid, accessible platform for objective motor and behavioural phenotyping in rodent models, with documented capabilities spanning locomotor activity, tremor quantification, ataxia assessment, and spatial behaviour analysis. The system achieves this functionality at approximately one-tenth the cost of commercial alternatives while maintaining measurement performance sufficient for detecting established motor phenotypes. Through open-source dissemination and community engagement, OpenStride has the potential to expand the use of force plate actometry across diverse research settings, contributing to more reproducible, quantitative, and high-throughput approaches to preclinical behavioural neuroscience.

5. References

- Anderson, C. J., Cadeddu, R., Anderson, D. N., Huxford, J. A., VanLuik, E. R., Odeh, K., Pittenger, C., Pulst, S. M., & Bortolato, M. (2024). A novel naïve Bayes approach to identifying grooming behaviors in the force-plate actometric platform. *Journal of Neuroscience Methods*, 403, 110026. <https://doi.org/https://doi.org/10.1016/j.jneumeth.2023.110026>
- Anderson, C. J., Figueroa, K. P., Dorval, A. D., & Pulst, S. M. (2019). Deep cerebellar stimulation reduces ataxic motor symptoms in the shaker rat. *Annals of Neurology*, 85(5), 681-690. <https://doi.org/https://doi.org/10.1002/ana.25464>
- Anderson, C. J., Figueroa, K. P., Paul, S., Gandelman, M., Dansithong, W., Katakowski, J. A., Scoles, D. R., & Pulst, S. M. (2025). Viral vector-mediated SLC9A6 gene replacement reduces cerebellar dysfunction in the shaker rat model of Christianson syndrome. *bioRxiv*. <https://doi.org/10.1101/2024.10.31.621435>
- Anderson, David J., & Perona, P. (2014). Toward a Science of Computational Ethology. *Neuron*, 84(1), 18-31. <https://doi.org/10.1016/j.neuron.2014.09.005>
- Baker, J. M. (2018). Gait Disorders. *Am J Med*, 131(6), 602-607. <https://doi.org/10.1016/j.amjmed.2017.11.051>
- Beltagui, A., Sesis, A., & Stylos, N. (2021). A bricolage perspective on democratising innovation: The case of 3D printing in makerspaces. *Technological Forecasting and Social Change*, 163, 120453. <https://doi.org/10.1016/j.techfore.2020.120453>
- Bidgood, R., Zubelzu, M., Ruiz-Ortega, J. A., & Morera-Herreras, T. (2024). Automated procedure to detect subtle motor alterations in the balance beam test in a mouse model of early Parkinson's disease. *Sci Rep*, 14(1), 862. <https://doi.org/10.1038/s41598-024-51225-1>
- Bobbert, M. F., & Schamhardt, H. C. (1990). Accuracy of determining the point of force application with piezoelectric force plates. *J Biomech*, 23(7), 705-710. [https://doi.org/10.1016/0021-9290\(90\)90169-4](https://doi.org/10.1016/0021-9290(90)90169-4)
- Bobic, O.-R., Sava, S. L., & Piele, A.-N. (2025). Makerspaces as Catalysts for Entrepreneurial Education: Insights from a Systematic Literature Review. *Education Sciences*.
- Brooks, S. P., & Dunnett, S. B. (2009). Tests to assess motor phenotype in mice: a user's guide. *Nature Reviews Neuroscience*, 10(7), 519-529. <https://doi.org/10.1038/nrn2652>
- Brownjohn, J. M. W., Pavic, A., & Omenzetter, P. (2004). A spectral density approach for modelling continuous vertical forces on pedestrian structures due to walking. *Canadian Journal of Civil Engineering*, 31(1), 65-77. <https://doi.org/10.1139/103-072>
- Butterworth, S. (1930). On the theory of filter amplifiers. *Wireless Engineer*, 7(6), 536-541.
- Button, K. S., Ioannidis, J. P. A., Mokrysz, C., Nosek, B. A., Flint, J., Robinson, E. S. J., & Munafò, M. R. (2013). Power failure: why small sample size undermines the reliability of neuroscience. *Nature Reviews Neuroscience*, 14(5), 365-376. <https://doi.org/10.1038/nrn3475>
- Carlezon, W. A., Jr., Duman, R. S., & Nestler, E. J. (2005). The many faces of CREB. *Trends Neurosci*, 28(8), 436-445. <https://doi.org/10.1016/j.tins.2005.06.005>
- Carter, R. J., Lione, L. A., Humby, T., Mangiarini, L., Mahal, A., Bates, G. P., Dunnett, S. B., & Morton, A. J. (1999). Characterization of progressive motor deficits in mice transgenic for the human Huntington's disease mutation. *J Neurosci*, 19(8), 3248-3257. <https://doi.org/10.1523/jneurosci.19-08-03248.1999>
- Carter, R. J., Morton, J., & Dunnett, S. B. (2001). Motor coordination and balance in rodents. *Curr Protoc Neurosci*, Chapter 8, Unit 8.12. <https://doi.org/10.1002/0471142301.ns0812s15>

- Cisek, P., & Green, A. M. (2024). Toward a neuroscience of natural behavior. *Current Opinion in Neurobiology*, 86, 102859. <https://doi.org/10.1016/j.conb.2024.102859>
- Crabbe, J. C., Wahlsten, D., & Dudek, B. C. (1999). Genetics of mouse behavior: interactions with laboratory environment. *Science*, 284(5420), 1670-1672. <https://doi.org/10.1126/science.284.5420.1670>
- Crawley, J. N. (2007). Mouse behavioral assays relevant to the symptoms of autism. *Brain Pathol*, 17(4), 448-459. <https://doi.org/10.1111/j.1750-3639.2007.00096.x>
- Crosland, K. A., Zarcone, J. R., Schroeder, S., Zarcone, T., & Fowler, S. (2005). Use of an Antecedent Analysis and a Force Sensitive Platform to Compare Stereotyped Movements and Motor Tics. *American Journal on Mental Retardation*, 110(3), 181-192. [https://doi.org/10.1352/0895-8017\(2005\)110<181:Uoaaaa>2.0.Co;2](https://doi.org/10.1352/0895-8017(2005)110<181:Uoaaaa>2.0.Co;2)
- Cryan, J. F., Markou, A., & Lucki, I. (2002). Assessing antidepressant activity in rodents: recent developments and future needs. *Trends Pharmacol Sci*, 23(5), 238-245. [https://doi.org/10.1016/s0165-6147\(02\)02017-5](https://doi.org/10.1016/s0165-6147(02)02017-5)
- de Assis, G. G., de Souza, E. O. N., de Almeida-Neto, P. F., Ceylan, H. İ., & Bragazzi, N. L. (2024). A Proposal for a Noxious Stimuli-Free, Moderate-Intensity Treadmill Running Protocol to Improve Aerobic Performance in Experimental Research on Rats. *Metabolites*, 14(10), 534. <https://www.mdpi.com/2218-1989/14/10/534>
- Deacon, R. M., & Rawlins, J. N. (2006). T-maze alternation in the rodent. *Nat Protoc*, 1(1), 7-12. <https://doi.org/10.1038/nprot.2006.2>
- Dijkhuizen, S., Van Ginneken, L. M. C., Ijpeelaar, A. H. C., Koekkoek, S. K. E., De Zeeuw, C. I., & Boele, H. J. (2024). Impact of enriched environment on motor performance and learning in mice. *Scientific Reports*, 14(1), 5962. <https://doi.org/10.1038/s41598-024-56568-3>
- Dunham, N. W., & Miya, T. S. (1957). A note on a simple apparatus for detecting neurological deficit in rats and mice. *J Am Pharm Assoc Am Pharm Assoc*, 46(3), 208-209. <https://doi.org/10.1002/jps.3030460322>
- Duty, S., & Jenner, P. (2011). Animal models of Parkinson's disease: a source of novel treatments and clues to the cause of the disease. *Br J Pharmacol*, 164(4), 1357-1391. <https://doi.org/10.1111/j.1476-5381.2011.01426.x>
- Farah, S., Anderson, D. G., & Langer, R. (2016). Physical and mechanical properties of PLA, and their functions in widespread applications — A comprehensive review. *Advanced Drug Delivery Reviews*, 107, 367-392. <https://doi.org/10.1016/j.addr.2016.06.012>
- Figuroa, K. P., Anderson, C. J., Paul, S., Dansithong, W., Gandelman, M., Scoles, D. R., & Pulst, S. M. (2023). Slc9a6 mutation causes Purkinje cell loss and ataxia in the shaker rat. *Human Molecular Genetics*, 32(10), 1647-1659. <https://doi.org/10.1093/hmg/ddad004>
- First, M. B. (2013). Diagnostic and statistical manual of mental disorders, 5th edition, and clinical utility. *J Nerv Ment Dis*, 201(9), 727-729. <https://doi.org/10.1097/NMD.0b013e3182a2168a>
- Fowler, S. C., Birkestrand, B., Chen, R., Vorontsova, E., & Zarcone, T. (2003). Behavioral sensitization to amphetamine in rats: changes in the rhythm of head movements during focused stereotypies. *Psychopharmacology*, 170(2), 167-177. <https://doi.org/10.1007/s00213-003-1528-5>
- Fowler, S. C., Birkestrand, B. R., Chen, R., Moss, S. J., Vorontsova, E., Wang, G., & Zarcone, T. J. (2001). A force-plate actometer for quantitating rodent behaviors: illustrative data on locomotion, rotation, spatial patterning, stereotypies, and tremor. *J Neurosci Methods*, 107(1-2), 107-124. [https://doi.org/10.1016/s0165-0270\(01\)00359-4](https://doi.org/10.1016/s0165-0270(01)00359-4)
- Fowler, S. C., Covington, H. E., 3rd, & Miczek, K. A. (2007). Stereotyped and complex motor routines expressed during cocaine self-administration: results from a 24-h binge of

- unlimited cocaine access in rats. *Psychopharmacology (Berl)*, 192(4), 465-478. <https://doi.org/10.1007/s00213-007-0739-6>
- Fowler, S. C., Pinkston, J., & Vorontsova, E. (2009). Timing and space usage are disrupted by amphetamine in rats maintained on DRL 24-s and DRL 72-s schedules of reinforcement. *Psychopharmacology (Berl)*, 204(2), 213-225. <https://doi.org/10.1007/s00213-008-1451-x>
- Fowler, S. C., Zarcone, T. J., Chen, R., Taylor, M. D., & Wright, D. E. (2002). Low grip strength, impaired tongue force and hyperactivity induced by overexpression of neurotrophin-3 in mouse skeletal muscle. *International Journal of Developmental Neuroscience*, 20(3), 303-308. [https://doi.org/10.1016/S0736-5748\(02\)00010-2](https://doi.org/10.1016/S0736-5748(02)00010-2)
- Fowler, S. C., Zarcone, T. J., & Levant, B. (2010). Methylphenidate attenuates rats' preference for a novel spatial stimulus introduced into a familiar environment: assessment using a force-plate actometer. *J Neurosci Methods*, 189(1), 36-43. <https://doi.org/10.1016/j.jneumeth.2010.03.014>
- Fowler, S. C., Zarcone, T. J., Vorontsova, E., & Chen, R. (2002). Motor and associative deficits in D2 dopamine receptor knockout mice. *International Journal of Developmental Neuroscience*, 20(3), 309-321. [https://doi.org/10.1016/S0736-5748\(02\)00009-6](https://doi.org/10.1016/S0736-5748(02)00009-6)
- Funato, T., Sato, Y., Sato, Y., Fujiki, S., Aoi, S., Tsuchiya, K., & Yanagihara, D. (2021). Quantitative evaluation of posture control in rats with inferior olive lesions. *Sci Rep*, 11(1), 20362. <https://doi.org/10.1038/s41598-021-99785-w>
- Gardner, W., Fuchs, F., Durieux, L., Bourgin, P., Coenen, V. A., Döbrössy, M., & Lecourtier, L. (2022). Slow Wave Sleep Deficits in the Flinders Sensitive Line Rodent Model of Depression: Effects of Medial Forebrain Bundle Deep-Brain Stimulation. *Neuroscience*, 498, 31-49. <https://doi.org/10.1016/j.neuroscience.2022.06.023>
- Gibson, L. J., & Ashby, M. F. (1997). *Cellular solids : structure and properties*. Cellular solids : structure and properties.
- Godar, S. C., Mosher, L. J., Strathman, H. J., Gochi, A. M., Jones, C. M., Fowler, S. C., & Bortolato, M. (2016). The D1CT-7 mouse model of Tourette syndrome displays sensorimotor gating deficits in response to spatial confinement. *British Journal of Pharmacology*, 173(13), 2111-2121. <https://doi.org/10.1111/bph.13243>
- Goetz, C. G., Tilley, B. C., Shaftman, S. R., Stebbins, G. T., Fahn, S., Martinez-Martin, P., Poewe, W., Sampaio, C., Stern, M. B., Dodel, R., Dubois, B., Holloway, R., Jankovic, J., Kulisevsky, J., Lang, A. E., Lees, A., Leurgans, S., LeWitt, P. A., Nyenhuis, D., . . . LaPelle, N. (2008). Movement Disorder Society-sponsored revision of the Unified Parkinson's Disease Rating Scale (MDS-UPDRS): scale presentation and clinimetric testing results. *Mov Disord*, 23(15), 2129-2170. <https://doi.org/10.1002/mds.22340>
- Guillot, T. S., Asress, S. A., Richardson, J. R., Glass, J. D., & Miller, G. W. (2008). Treadmill gait analysis does not detect motor deficits in animal models of Parkinson's disease or amyotrophic lateral sclerosis. *J Mot Behav*, 40(6), 568-577. <https://doi.org/10.3200/jmbr.40.6.568-577>
- Gururajan, A., Reif, A., Cryan, J. F., & Slattery, D. A. (2019). The future of rodent models in depression research. *Nature Reviews Neuroscience*, 20(11), 686-701. <https://doi.org/10.1038/s41583-019-0221-6>
- Handforth, A., & Krahl, S. E. (2001). Suppression of harmaline-induced tremor in rats by vagus nerve stimulation. *Mov Disord*, 16(1), 84-88. [https://doi.org/10.1002/1531-8257\(200101\)16:1<84::aid-mds1010>3.0.co;2-s](https://doi.org/10.1002/1531-8257(200101)16:1<84::aid-mds1010>3.0.co;2-s)
- Hansen, S. T., & Pulst, S. M. (2013). Response to ethanol induced ataxia between C57BL/6J and 129X1/SvJ mouse strains using a treadmill based assay. *Pharmacol Biochem Behav*, 103(3), 582-588. <https://doi.org/10.1016/j.pbb.2012.10.010>

- Harnie, J., Doelman, A., de Vette, E., Audet, J., Desrochers, E., Gaudreault, N., & Frigon, A. (2019). The recovery of standing and locomotion after spinal cord injury does not require task-specific training. *Elife*, 8. <https://doi.org/10.7554/eLife.50134>
- Hein, A. M., Zarcone, T. J., Parfitt, D. B., Matousek, S. B., Carbonari, D. M., Olschowka, J. A., & O'Banion, M. K. (2012). Behavioral, structural and molecular changes following long-term hippocampal IL-1 β overexpression in transgenic mice. *J Neuroimmune Pharmacol*, 7(1), 145-155. <https://doi.org/10.1007/s11481-011-9294-3>
- Herbin, M., Hackert, R., Gasc, J. P., & Renous, S. (2007). Gait parameters of treadmill versus overground locomotion in mouse. *Behav Brain Res*, 181(2), 173-179. <https://doi.org/10.1016/j.bbr.2007.04.001>
- Hövel, F. F. V., Leiter, I., Rumpel, R., Langenhagen, A., Wedekind, D., Häger, C., Bleich, A., Palme, R., & Grothe, C. (2019). FGF-2 isoforms influence the development of dopaminergic neurons in the murine substantia nigra, but not anxiety-like behavior, stress susceptibility, or locomotor behavior. *Behav Brain Res*, 374, 112113. <https://doi.org/10.1016/j.bbr.2019.112113>
- Isik, S., & Unal, G. (2023). Open-source software for automated rodent behavioral analysis. *Front Neurosci*, 17, 1149027. <https://doi.org/10.3389/fnins.2023.1149027>
- Jafari, Z., Kolb, B. E., & Mohajerani, M. H. (2020). Prepulse inhibition of the acoustic startle reflex and P50 gating in aging and alzheimer's disease. *Ageing Research Reviews*, 59, 101028. <https://doi.org/10.1016/j.arr.2020.101028>
- Jones, B. J., & Roberts, D. J. (1968). The quantitative measurement of motor inco-ordination in naive mice using an accelerating rotarod. *J Pharm Pharmacol*, 20(4), 302-304. <https://doi.org/10.1111/j.2042-7158.1968.tb09743.x>
- Kafkafi, N., Benjamini, Y., Sakov, A., Elmer, G. I., & Golani, I. (2005). Genotype-environment interactions in mouse behavior: a way out of the problem. *Proc Natl Acad Sci U S A*, 102(12), 4619-4624. <https://doi.org/10.1073/pnas.0409554102>
- Kilts, C. D. (2001). The changing roles and targets for animal models of schizophrenia. *Biological Psychiatry*, 50(11), 845-855. [https://doi.org/10.1016/S0006-3223\(01\)01286-0](https://doi.org/10.1016/S0006-3223(01)01286-0)
- Kohl, S., Heekeren, K., Klosterkötter, J., & Kuhn, J. (2013). Prepulse inhibition in psychiatric disorders – Apart from schizophrenia. *Journal of Psychiatric Research*, 47(4), 445-452. <https://doi.org/10.1016/j.jpsychires.2012.11.018>
- Krishnan, V., Han, M. H., Graham, D. L., Berton, O., Renthal, W., Russo, S. J., Laplant, Q., Graham, A., Lutter, M., Lagace, D. C., Ghose, S., Reister, R., Tannous, P., Green, T. A., Neve, R. L., Chakravarty, S., Kumar, A., Eisch, A. J., Self, D. W., . . . Nestler, E. J. (2007). Molecular adaptations underlying susceptibility and resistance to social defeat in brain reward regions. *Cell*, 131(2), 391-404. <https://doi.org/10.1016/j.cell.2007.09.018>
- Kuo, S.-H., Louis, E. D., Faust, P. L., Handforth, A., Chang, S.-y., Avlar, B., Lang, E. J., Pan, M.-K., Miterko, L. N., Brown, A. M., Sillitoe, R. V., Anderson, C. J., Pulst, S. M., Gallagher, M. J., Lyman, K. A., Chetkovich, D. M., Clark, L. N., Tio, M., Tan, E.-K., & Elble, R. J. (2019). Current Opinions and Consensus for Studying Tremor in Animal Models. *The Cerebellum*, 18(6), 1036-1063. <https://doi.org/10.1007/s12311-019-01037-1>
- Lalonde, R. (2002). The neurobiological basis of spontaneous alternation. *Neurosci Biobehav Rev*, 26(1), 91-104. [https://doi.org/10.1016/s0149-7634\(01\)00041-0](https://doi.org/10.1016/s0149-7634(01)00041-0)
- Lang, J., Haas, E., Hübener-Schmid, J., Anderson, C. J., Pulst, S. M., Giese, M. A., & Ilg, W. (2020, 20-24 July 2020). Detecting and Quantifying Ataxia-Related Motor Impairments in Rodents Using Markerless Motion Tracking With Deep Neural Networks. 2020 42nd Annual International Conference of the IEEE Engineering in

<https://doi.org/10.1109/EMBC44109.2020.9176701>,

- Levant, B., Zarcone, T. J., Davis, P. F., Ozias, M. K., & Fowler, S. C. (2011). Differences in methylphenidate dose response between periadolescent and adult rats in the familiar arena-novel alcove task. *J Pharmacol Exp Ther*, 337(1), 83-91. <https://doi.org/10.1124/jpet.110.174425>
- Levant, B., Zarcone, T. J., & Fowler, S. C. (2010). Developmental effects of dietary n-3 fatty acids on activity and response to novelty. *Physiol Behav*, 101(1), 176-183. <https://doi.org/10.1016/j.physbeh.2010.04.038>
- Levitis, D. A., Lidicker, W. Z., & Freund, G. (2009). Behavioural biologists do not agree on what constitutes behaviour. *Animal Behaviour*, 78(1), 103-110. <https://doi.org/10.1016/j.anbehav.2009.03.018>
- Luong, T. N., Carlisle, H. J., Southwell, A., & Patterson, P. H. (2011). Assessment of motor balance and coordination in mice using the balance beam. *J Vis Exp*(49). <https://doi.org/10.3791/2376>
- Maier, I. C., Ichiyama, R. M., Courtine, G., Schnell, L., Lavrov, I., Edgerton, V. R., & Schwab, M. E. (2009). Differential effects of anti-Nogo-A antibody treatment and treadmill training in rats with incomplete spinal cord injury. *Brain*, 132(Pt 6), 1426-1440. <https://doi.org/10.1093/brain/awp085>
- Mathis, A., Mamidanna, P., Cury, K. M., Abe, T., Murthy, V. N., Mathis, M. W., & Bethge, M. (2018). DeepLabCut: markerless pose estimation of user-defined body parts with deep learning. *Nat Neurosci*, 21(9), 1281-1289. <https://doi.org/10.1038/s41593-018-0209-y>
- Mathis, A., Schneider, S., Lauer, J., & Mathis, M. W. (2020). A Primer on Motion Capture with Deep Learning: Principles, Pitfalls, and Perspectives. *Neuron*, 108(1), 44-65. <https://doi.org/10.1016/j.neuron.2020.09.017>
- McCarson, K. E., Winter, M. K., Abrahamson, D. R., Berman, N. E., & Smith, P. G. (2019). Assessing complex movement behaviors in rodent models of neurological disorders. *Neurobiol Learn Mem*, 165, 106817. <https://doi.org/10.1016/j.nlm.2018.02.025>
- McCullough, M. H., & Goodhill, G. J. (2021). Unsupervised quantification of naturalistic animal behaviors for gaining insight into the brain. *Current Opinion in Neurobiology*, 70, 89-100. <https://doi.org/10.1016/j.conb.2021.07.014>
- McFadyen, M. P., Kusek, G., Bolivar, V. J., & Flaherty, L. (2003). Differences among eight inbred strains of mice in motor ability and motor learning on a rotorod. *Genes Brain Behav*, 2(4), 214-219. <https://doi.org/10.1034/j.1601-183x.2003.00028.x>
- Metz, G. A., & Whishaw, I. Q. (2002). Cortical and subcortical lesions impair skilled walking in the ladder rung walking test: a new task to evaluate fore- and hindlimb stepping, placing, and co-ordination. *J Neurosci Methods*, 115(2), 169-179. [https://doi.org/10.1016/s0165-0270\(02\)00012-2](https://doi.org/10.1016/s0165-0270(02)00012-2)
- Middleton, J., Sinclair, P., & Patton, R. (1999). Accuracy of centre of pressure measurement using a piezoelectric force platform. *Clin Biomech (Bristol)*, 14(5), 357-360. [https://doi.org/10.1016/s0268-0033\(98\)00079-5](https://doi.org/10.1016/s0268-0033(98)00079-5)
- Mosher, L. J., Cadeddu, R., Yen, S., Staudinger, J. L., Traccis, F., Fowler, S. C., Maguire, J. L., & Bortolato, M. (2019). Allopregnanolone is required for prepulse inhibition deficits induced by D1 dopamine receptor activation. *Psychoneuroendocrinology*, 108, 53-61. <https://doi.org/https://doi.org/10.1016/j.psyneuen.2019.06.009>
- Mosher, L. J., Godar, S. C., Morissette, M., McFarlin, K. M., Scheggi, S., Gambarana, C., Fowler, S. C., Di Paolo, T., & Bortolato, M. (2018). Steroid 5 α -reductase 2 deficiency leads to reduced dominance-related and impulse-control behaviors.

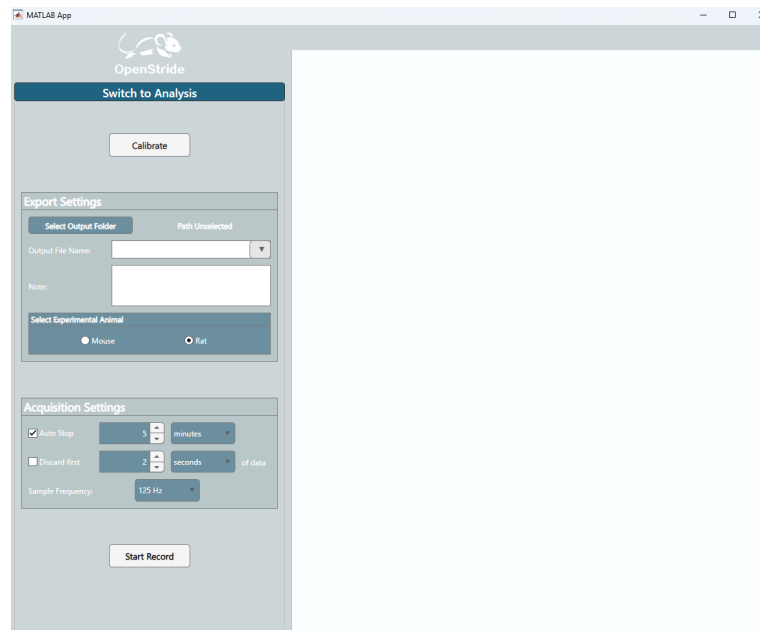
- <https://doi.org/https://doi.org/10.1016/j.psyneuen.2018.02.007>
- Namdar, I., Feldman, R., Glazer, S., Meninger, I., Shlobin, N. A., Rubovitch, V., Bikovski, L., Been, E., & Pick, C. G. (2020). Motor Effects of Minimal Traumatic Brain Injury in Mice. *J Mol Neurosci*, 70(3), 365-377. <https://doi.org/10.1007/s12031-019-01422-9>
- Neckel, N. D., Blonien, N., Nichols, D., & Hidler, J. (2008). Abnormal joint torque patterns exhibited by chronic stroke subjects while walking with a prescribed physiological gait pattern. *J Neuroeng Rehabil*, 5, 19. <https://doi.org/10.1186/1743-0003-5-19>
- Nestler, E. J., & Hyman, S. E. (2010). Animal models of neuropsychiatric disorders. *Nat Neurosci*, 13(10), 1161-1169. <https://doi.org/10.1038/nn.2647>
- Noldus, L. P., Spink, A. J., & Tegelenbosch, R. A. (2001). EthoVision: a versatile video tracking system for automation of behavioral experiments. *Behav Res Methods Instrum Comput*, 33(3), 398-414. <https://doi.org/10.3758/bf03195394>
- Pearce, J. M. (2012). Building Research Equipment with Free, Open-Source Hardware. *Science*, 337(6100), 1303-1304. <https://doi.org/doi:10.1126/science.1228183>
- Pereira, T. D., Shaevitz, J. W., & Murthy, M. (2020). Quantifying behavior to understand the brain. *Nature Neuroscience*, 23(12), 1537-1549. <https://doi.org/10.1038/s41593-020-00734-z>
- Pereira, T. D., Tabris, N., Matsliah, A., Turner, D. M., Li, J., Ravindranath, S., Papadoyannis, E. S., Normand, E., Deutsch, D. S., Wang, Z. Y., McKenzie-Smith, G. C., Mitelut, C. C., Castro, M. D., D'Uva, J., Kislin, M., Sanes, D. H., Kocher, S. D., Wang, S. S., Falkner, A. L., . . . Murthy, M. (2022). SLEAP: A deep learning system for multi-animal pose tracking. *Nat Methods*, 19(4), 486-495. <https://doi.org/10.1038/s41592-022-01426-1>
- Perrin, S. (2014). Preclinical research: Make mouse studies work. *Nature*, 507(7493), 423-425. <https://doi.org/10.1038/507423a>
- Pinkston, J. W., Madden, G. J., & Fowler, S. C. (2008). Effects of white and infrared lighting on apomorphine-induced pecking in pigeons. *Behavioural Pharmacology*, 19(4), 347-352. <https://doi.org/10.1097/FBP.0b013e32830990ac>
- Piotrowski, D., Clemensson, E. K. H., Nguyen, H. P., & Mark, M. D. (2024). Phenotypic analysis of ataxia in spinocerebellar ataxia type 6 mice using DeepLabCut. *Sci Rep*, 14(1), 8571. <https://doi.org/10.1038/s41598-024-59187-0>
- Porsolt, R. D., Le Pichon, M., & Jalfre, M. (1977). Depression: a new animal model sensitive to antidepressant treatments. *Nature*, 266(5604), 730-732. <https://doi.org/10.1038/266730a0>
- Russell, K. L., Berman, N. E., & Levant, B. (2013). Low brain DHA content worsens sensorimotor outcomes after TBI and decreases TBI-induced Timp1 expression in juvenile rats. *Prostaglandins Leukot Essent Fatty Acids*, 89(2-3), 97-105. <https://doi.org/10.1016/j.plefa.2013.05.004>
- Rustay, N. R., Wahlsten, D., & Crabbe, J. C. (2003). Influence of task parameters on rotarod performance and sensitivity to ethanol in mice. *Behav Brain Res*, 141(2), 237-249. [https://doi.org/10.1016/s0166-4328\(02\)00376-5](https://doi.org/10.1016/s0166-4328(02)00376-5)
- Sagvolden, T., Johansen, E. B., Aase, H., & Russell, V. A. (2005). A dynamic developmental theory of attention-deficit/hyperactivity disorder (ADHD) predominantly hyperactive/impulsive and combined subtypes. *Behav Brain Sci*, 28(3), 397-419; discussion 419-368. <https://doi.org/10.1017/s0140525x05000075>
- Sathyasesan, A., & Gallo, V. (2019). Cerebellar contribution to locomotor behavior: A neurodevelopmental perspective. *Neurobiol Learn Mem*, 165, 106861. <https://doi.org/10.1016/j.nlm.2018.04.016>

- Savitzky, A., & Golay, M. J. (1964). Smoothing and differentiation of data by simplified least squares procedures. *Analytical chemistry*, 36(8), 1627-1639.
- Sawers, A., & Ting, L. H. (2015). Beam walking can detect differences in walking balance proficiency across a range of sensorimotor abilities. *Gait Posture*, 41(2), 619-623. <https://doi.org/10.1016/j.gaitpost.2015.01.007>
- Scoles, D. R., Paul, S., Dansithong, W., Figueroa, K. P., Gandelman, M., Royzen, F., Anderson, C. J., & Pulst, S. M. (2022). Targeting Staufen 1 with antisense oligonucleotides for treating ALS and SCA2. *bioRxiv*, 2022.2011.2016.516816. <https://doi.org/10.1101/2022.11.16.516816>
- Shmelkov, S. V., Hormigo, A., Jing, D., Proenca, C. C., Bath, K. G., Milde, T., Shmelkov, E., Kushner, J. S., Baljevic, M., Dincheva, I., Murphy, A. J., Valenzuela, D. M., Gale, N. W., Yancopoulos, G. D., Ninan, I., Lee, F. S., & Rafii, S. (2010). Slitrk5 deficiency impairs corticostriatal circuitry and leads to obsessive-compulsive-like behaviors in mice. *Nat Med*, 16(5), 598-602, 591p following 602. <https://doi.org/10.1038/nm.2125>
- Steru, L., Chermat, R., Thierry, B., & Simon, P. (1985). The tail suspension test: a new method for screening antidepressants in mice. *Psychopharmacology (Berl)*, 85(3), 367-370. <https://doi.org/10.1007/bf00428203>
- Sturman, O., von Ziegler, L., Schläppi, C., Akyol, F., Privitera, M., Slominski, D., Grimm, C., Thieren, L., Zerbi, V., Grewe, B., & Bohacek, J. (2020). Deep learning-based behavioral analysis reaches human accuracy and is capable of outperforming commercial solutions. *Neuropsychopharmacology*, 45(11), 1942-1952. <https://doi.org/10.1038/s41386-020-0776-y>
- Swerdlow, N. R. (2013). Update: studies of prepulse inhibition of startle, with particular relevance to the pathophysiology or treatment of Tourette Syndrome. *Neurosci Biobehav Rev*, 37(6), 1150-1156. <https://doi.org/10.1016/j.neubiorev.2012.09.002>
- Swerdlow, N. R., Braff, D. L., Taaid, N., & Geyer, M. A. (1994). Assessing the validity of an animal model of deficient sensorimotor gating in schizophrenic patients. *Arch Gen Psychiatry*, 51(2), 139-154. <https://doi.org/10.1001/archpsyc.1994.03950020063007>
- Swerdlow, N. R., Weber, M., Qu, Y., Light, G. A., & Braff, D. L. (2008). Realistic expectations of prepulse inhibition in translational models for schizophrenia research. *Psychopharmacology (Berl)*, 199(3), 331-388. <https://doi.org/10.1007/s00213-008-1072-4>
- Tanner, C. M., & Ostrem, J. L. (2024). Parkinson's Disease. *N Engl J Med*, 391(5), 442-452. <https://doi.org/10.1056/NEJMra2401857>
- Tao, R., Shokry, I. M., Callanan, J. J., Adams, H. D., & Ma, Z. (2015). Mechanisms and environmental factors that underlying the intensification of 3,4-methylenedioxymethamphetamine (MDMA, Ecstasy)-induced serotonin syndrome in rats. *Psychopharmacology (Berl)*, 232(7), 1245-1260. <https://doi.org/10.1007/s00213-014-3759-z>
- Taylor, J. R., Morshed, S. A., Parveen, S., Mercadante, M. T., Scahill, L., Peterson, B. S., King, R. A., Leckman, J. F., & Lombroso, P. J. (2002). An animal model of Tourette's syndrome. *Am J Psychiatry*, 159(4), 657-660. <https://doi.org/10.1176/appi.ajp.159.4.657>
- Tejwani, L., Ravindra, N. G., Lee, C., Cheng, Y., Nguyen, B., Luttik, K., Ni, L., Zhang, S., Morrison, L. M., Gionco, J., Xiang, Y., Yoon, J., Ro, H., Haidery, F., Grijalva, R. M., Bae, E., Kim, K., Martuscello, R. T., Orr, H. T., . . . Lim, J. (2024). Longitudinal single-cell transcriptional dynamics throughout neurodegeneration in SCA1. *Neuron*, 112(3), 362-383.e315. <https://doi.org/10.1016/j.neuron.2023.10.039>
- Tickerhoof, M. C., Hale, L. H., Butler, M. J., & Smith, A. S. (2020). Regulation of defeat-induced social avoidance by medial amygdala DRD1 in male and female prairie voles.

- <https://doi.org/https://doi.org/10.1016/j.psyneuen.2019.104542>
- Vandeputte, C., Taymans, J. M., Casteels, C., Coun, F., Ni, Y., Van Laere, K., & Baekelandt, V. (2010). Automated quantitative gait analysis in animal models of movement disorders. *BMC Neurosci*, *11*, 92. <https://doi.org/10.1186/1471-2202-11-92>
- Vinueza Veloz, M. F., Buijsen, R. A., Willemsen, R., Cupido, A., Bosman, L. W., Koekkoek, S. K., Potters, J. W., Oostra, B. A., & De Zeeuw, C. I. (2012). The effect of an mGluR5 inhibitor on procedural memory and avoidance discrimination impairments in Fmr1 KO mice. *Genes Brain Behav*, *11*(3), 325-331. <https://doi.org/10.1111/j.1601-183X.2011.00763.x>
- Vinueza Veloz, M. F., Zhou, K., Bosman, L. W., Potters, J. W., Negrello, M., Seepers, R. M., Strydis, C., Koekkoek, S. K., & De Zeeuw, C. I. (2015). Cerebellar control of gait and interlimb coordination. *Brain Struct Funct*, *220*(6), 3513-3536. <https://doi.org/10.1007/s00429-014-0870-1>
- von Ziegler, L., Sturman, O., & Bohacek, J. (2021). Big behavior: challenges and opportunities in a new era of deep behavior profiling. *Neuropsychopharmacology*, *46*(1), 33-44. <https://doi.org/10.1038/s41386-020-0751-7>
- Wallace, D. L., Han, M. H., Graham, D. L., Green, T. A., Vialou, V., Iñiguez, S. D., Cao, J. L., Kirk, A., Chakravarty, S., Kumar, A., Krishnan, V., Neve, R. L., Cooper, D. C., Bolaños, C. A., Barrot, M., McClung, C. A., & Nestler, E. J. (2009). CREB regulation of nucleus accumbens excitability mediates social isolation-induced behavioral deficits. *Nat Neurosci*, *12*(2), 200-209. <https://doi.org/10.1038/nn.2257>
- Wang, Y. M., Liu, C. W., Chen, S. Y., Lu, L. Y., Liu, W. C., Wang, J. H., Ni, C. L., Wong, S. B., Kumar, A., Lee, J. C., Kuo, S. H., Wu, S. C., & Pan, M. K. (2024). Neuronal population activity in the olivocerebellum encodes the frequency of essential tremor in mice and patients. *Sci Transl Med*, *16*(747), ead11408. <https://doi.org/10.1126/scitranslmed.adl1408>
- Welch, J. M., Lu, J., Rodriguiz, R. M., Trotta, N. C., Peca, J., Ding, J.-D., Feliciano, C., Chen, M., Adams, J. P., Luo, J., Dudek, S. M., Weinberg, R. J., Calakos, N., Wetsel, W. C., & Feng, G. (2007). Cortico-striatal synaptic defects and OCD-like behaviours in Sapap3-mutant mice. *Nature*, *448*(7156), 894-900. <https://doi.org/10.1038/nature06104>
- Welton, T., Cardoso, F., Carr, J. A., Chan, L.-L., Deuschl, G., Jankovic, J., & Tan, E.-K. (2021). Essential tremor. *Nature Reviews Disease Primers*, *7*(1), 83. <https://doi.org/10.1038/s41572-021-00314-w>
- Wheeler, G. E., Purkayastha, A., Bunker, E. N., Bortz, D. M., & Liu, X. (2021). Protocol for Analysis and Consolidation of TrackMate Outputs for Measuring Two-Dimensional Cell Motility using Nuclear Tracking. *J Vis Exp*(178). <https://doi.org/10.3791/62885>
- Wooley, C. M., Sher, R. B., Kale, A., Frankel, W. N., Cox, G. A., & Seburn, K. L. (2005). Gait analysis detects early changes in transgenic SOD1(G93A) mice. *Muscle Nerve*, *32*(1), 43-50. <https://doi.org/10.1002/mus.20228>
- Zarcone, T. J. (2022). Neuroscience and actometry: An example of the benefits of the precise measurement of behavior. *Brain Res Bull*, *185*, 86-90. <https://doi.org/10.1016/j.brainresbull.2022.04.009>
- Zarcone, T. J., Chen, R., & Fowler, S. C. (2009). Effects of differing response-force requirements on food-maintained responding in C57Bl/6J mice. *J Exp Anal Behav*, *92*(2), 257-274. <https://doi.org/10.1901/jeab.2009.92-257>

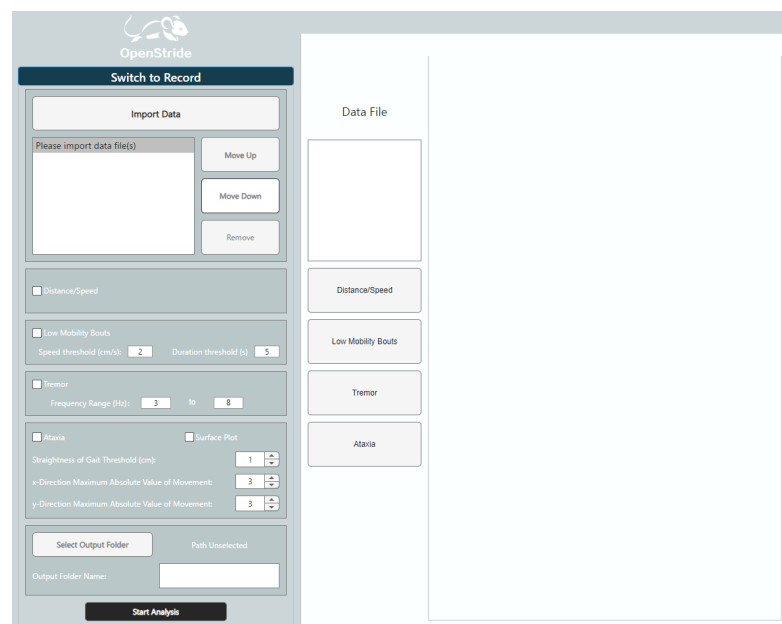
Appendix A

Figure A.1 OpenStride graphical user interface (main window)



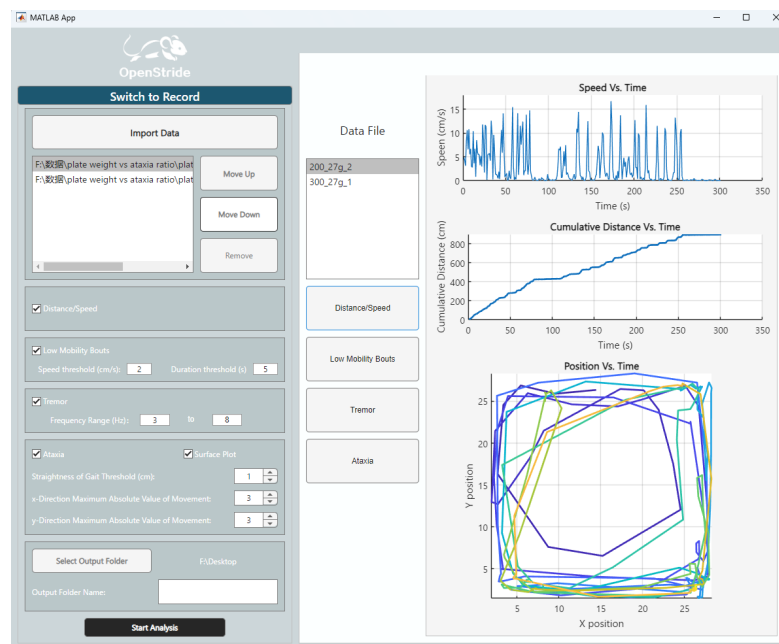
The main control window of OpenStride, providing access to data acquisition, configuration settings, and analysis modules.

Figure A.2 OpenStride data analysis interface



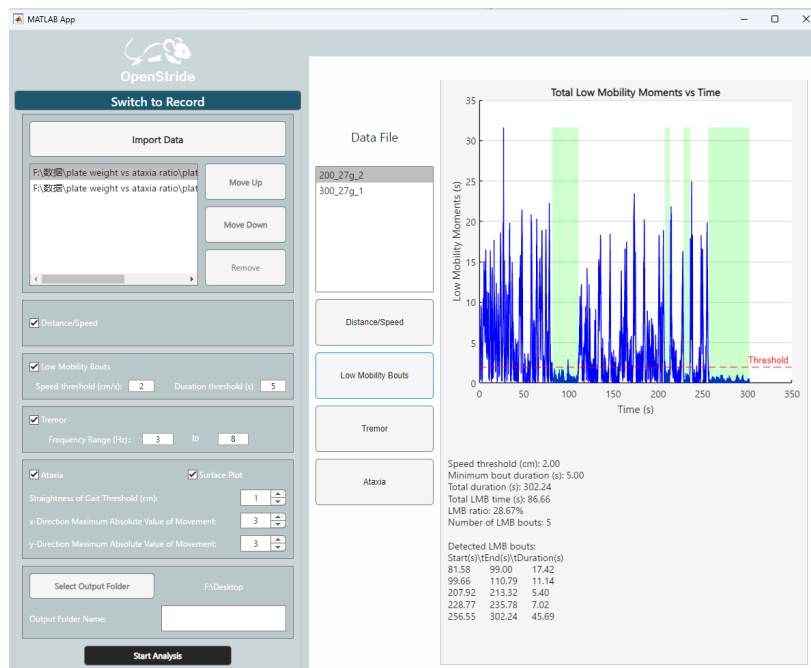
The analysis interface for loading, managing, and processing recorded datasets, including file selection and parameter configuration.

Figure A.3 Distance and speed analysis results



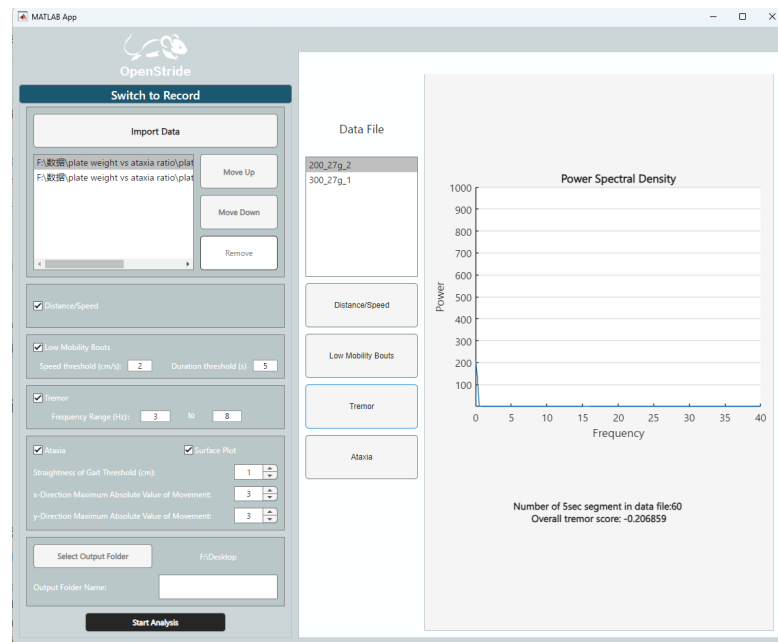
Visualization of locomotor activity, showing distance traveled and speed profiles over time.

Figure A.4 LMB analysis results



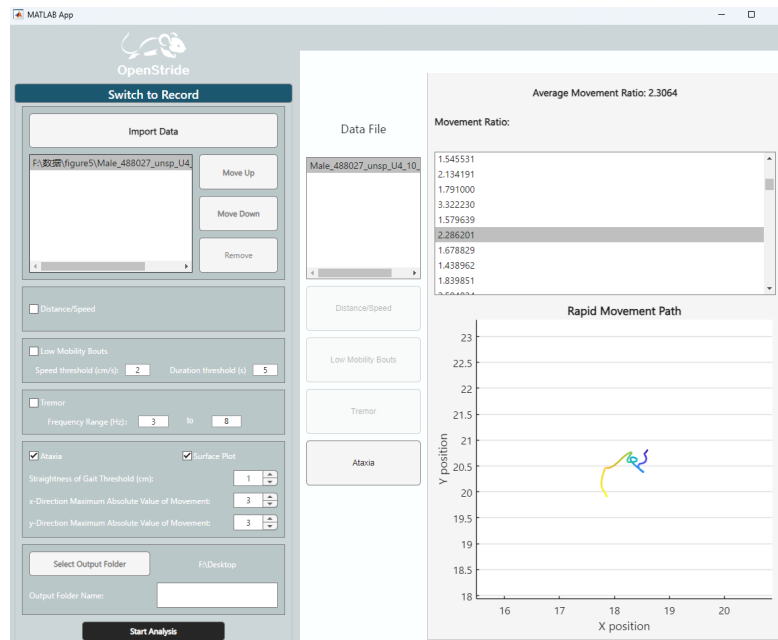
Output of locomotor behavioral metrics (LMB), summarizing movement patterns and behavioral segmentation based on algorithmic classification.

Figure A.5 Tremor analysis results



Spectral and time-domain analysis results used to quantify tremor-related activity and oscillatory movement features.

Figure A.6 Ataxia analysis results



Quantitative assessment of ataxia-related motor impairment, including instability metrics and coordination-related movement parameters.

Code Availability and Software Documentation

The OpenStride platform is supported by custom software developed by the author using Python and MATLAB. These programs implement data acquisition, calibration, signal processing, behavioural analysis, and graphical user interface functionality described in this thesis.

In accordance with current open-science practices, the full source code for all software and all files for hardware replication have been made publicly available at <https://github.com/OpenStrideNeuro/OpenStride>.